

2016 CROSCUTTING RESEARCH AND RARE EARTH ELEMENTS PORTFOLIOS REVIEW
Pittsburgh, PA, April 18–22, 2016

Novel Functional Graded Thermal Barrier Coatings in Coal-fired Power Plant Turbines

Jing Zhang

Department of Mechanical Engineering
Indiana University-Purdue University Indianapolis

Grant No.: DOE DE-FE0008868
Program Manager: Richard Dunst

IUPUI

INDIANA UNIVERSITY
PURDUE UNIVERSITY
INDIANAPOLIS

Acknowledgement



- Subcontract: James Knapp (Praxair Surface Technologies)
- Collaborators: Li Li, Don Lemen (Praxair Surface Technologies)
- Yeon-Gil Jung (Changwon National University), Ungyu Paik (Hanyang University)
- Yang Ren, Jiangang Sun (Argonne National Laboratory)
- Changdong Wei (OSU), Bin Hu (Dartmouth)
- Ph.D. graduate students: Xingye Guo, Yi Zhang

Outline

- Introduction
- Coating design and fabrication
 - Single ceramic layer (SCL) & Double ceramic layer (DCL) architectures
 - Composite coatings with buffer layers
- Characterization of physical and mechanical properties
 - Microstructure and composition
 - Porosity and hardness
 - Bond strength test
 - Erosion test
- Characterization of thermal property and thermal durability
 - Thermal conductivity, specific heat, coeff. of thermal expansion
 - Thermal shock (TS) test
 - Jet engine thermal shock (JETS) test
 - Furnace cycling thermal fatigue (FCTF) test
 - Thermal gradient mechanical fatigue (TGMF) test
- MD&FE modeling of thermal conductivity; DFT calculation of gas adsorption
- Summary and future work

Limitation of yttria stabilized zirconia

Zirconia partially stabilized with 7~8 wt% yttria (YSZ) is the current state-of-the-art thermal barrier coating material.

The thermal conductivity of 8YSZ is ~2.12 W/m-K @ 800°C. **Lower thermal conductivity materials are required** for future gas turbines.

Above 1200 °C, YSZ **transforms** from t' phase to the tetragonal and cubic phase (*t* and *c* phases, respectively) during cooling process, and then to monoclinic (*m*) phase with a volume expansion of about 3–5 vol.%, resulting in the spallation or delamination of TBCs.

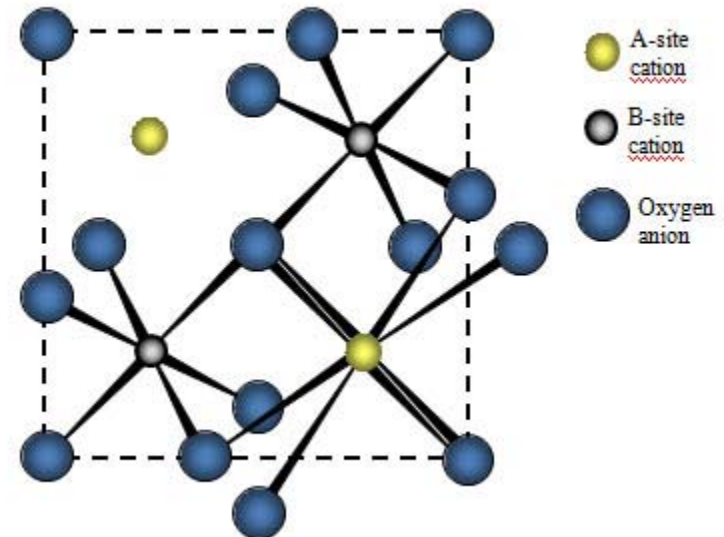
Additionally, at temperatures above 1200 °C, YSZ layers are prone to **sintering**, which increases thermal conductivity and makes them less effective. The sintered and densified coatings can also **reduce thermal stress and strain tolerance**, which can reduce the coating's durability significantly.

Motivation and objective

- To further increase the operating temperatures of turbine engines, alternative TBC materials with lower thermal conductivity, higher thermal stability and better sintering resistance are required.
- The objective of the project is to develop a novel lanthanum zirconate ($\text{La}_2\text{Zr}_2\text{O}_7$) based multi-layer thermal barrier coating system.
- The ultimate goal is to develop a manufacturing process to produce pyrochlore oxide based coatings with improved high-temperature properties.

Pyrochlore - $A_2B_2O_7$

Pyrochlore-type rare earth zirconium oxides ($(Re_2Zr_2O_7$, Re = rare earth) are promising candidates for thermal barrier coatings, high-permittivity dielectrics, potential solid electrolytes in high-temperature fuel cells, and immobilization hosts of actinides in nuclear waste.

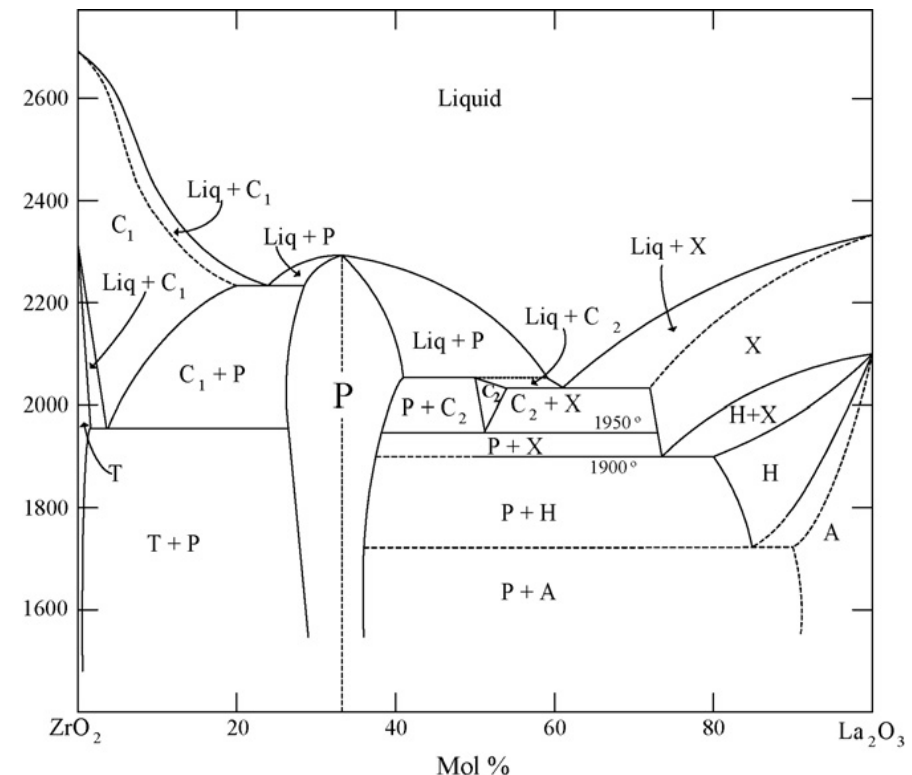


Pyrochlore crystal structure:
 $A_2B_2O_7$. A and B are metals incorporated into the structure in various combinations. (credit: NETL)

Why $\text{La}_2\text{Zr}_2\text{O}_7$?

Compared with YSZ, $\text{La}_2\text{Zr}_2\text{O}_7$ has

- Lower thermal conductivity
- Higher temperature phase stability. No phase transformation
- Lower sintering rate at elevated temperatures
- Lower CTE



Phase diagram of $\text{La}_2\text{O}_3-\text{ZrO}_2$

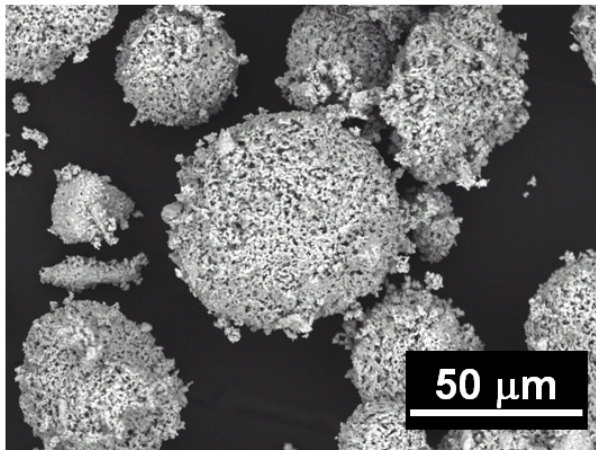
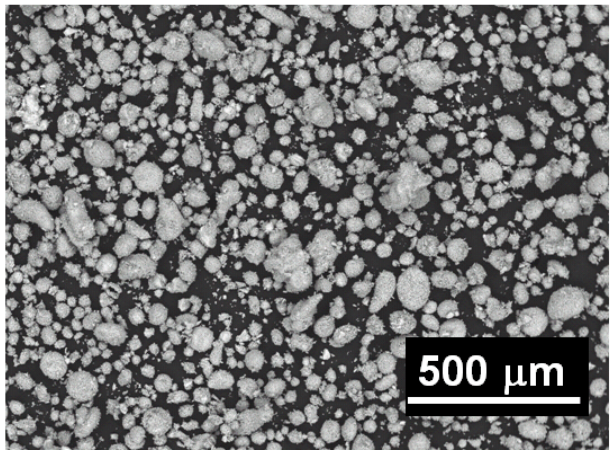
La₂Zr₂O₇ vs. YSZ

Materials property	8YSZ	La₂Zr₂O₇
Melting Point (°C)	2680	2300
Maximum Operating Temperature (°C)	1200	>1300
Thermal Conductivity (W/m-K) (@ 800°C)	2.12	1.6
Coefficient of Thermal Expansion (x10 ⁻⁶ /°C) (@1000 °C)	11.0	8.9-9.1
Density (g/cm ³)	6.07	6.00
Specific heat (J/g-°C) (@1000 °C)	0.64	0.54

Layered coating architecture

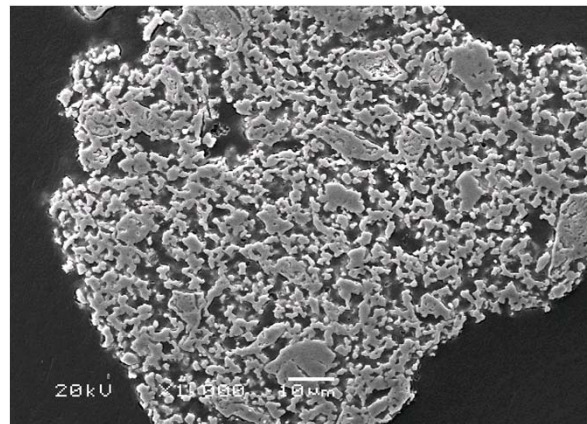
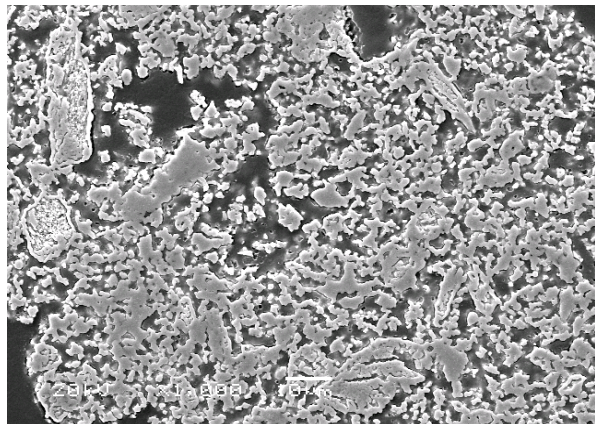
- The coefficient of thermal expansion of $\text{La}_2\text{Zr}_2\text{O}_7$ ($\sim 9 \times 10^{-6} /^\circ\text{C}$) is lower than those of both substrate and bondcoat ($\sim 15 \times 10^{-6} /^\circ\text{C}$ @ 1000 °C). As a result, the thermal cycling properties may be a concern
- The layered topcoat architecture is believed to be a feasible solution to improve thermal strain tolerance
- In this work, we develop multi-layer, compositionally graded, pyrochlore oxide based TBC systems

$\text{La}_2\text{Zr}_2\text{O}_7$ spray powder morphology



Powder surface morphology

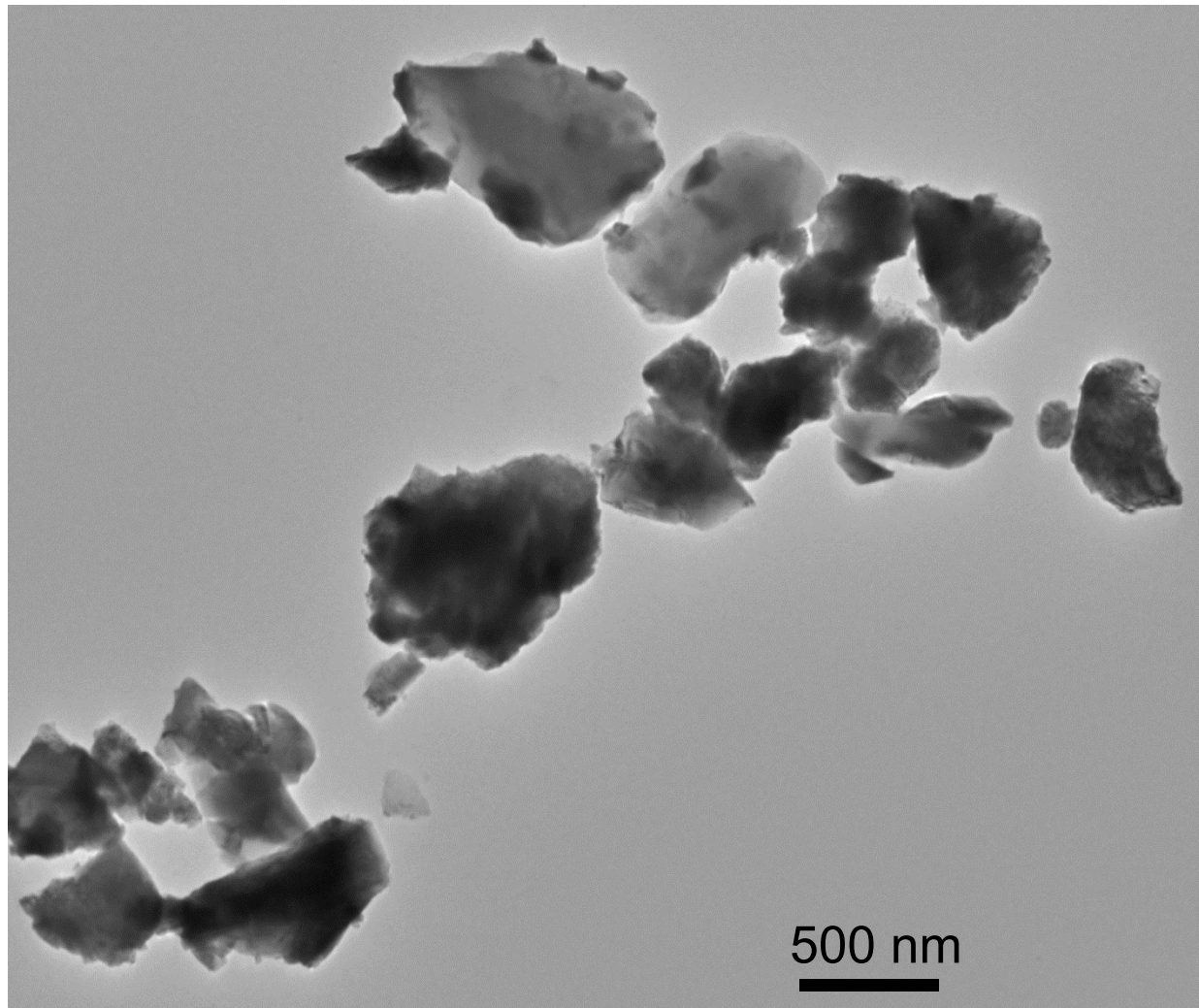
- Spherical shape with a rough surface
- Good flowability and high density
- Particle size between 30 ~ 100 μm



Powder cross-section

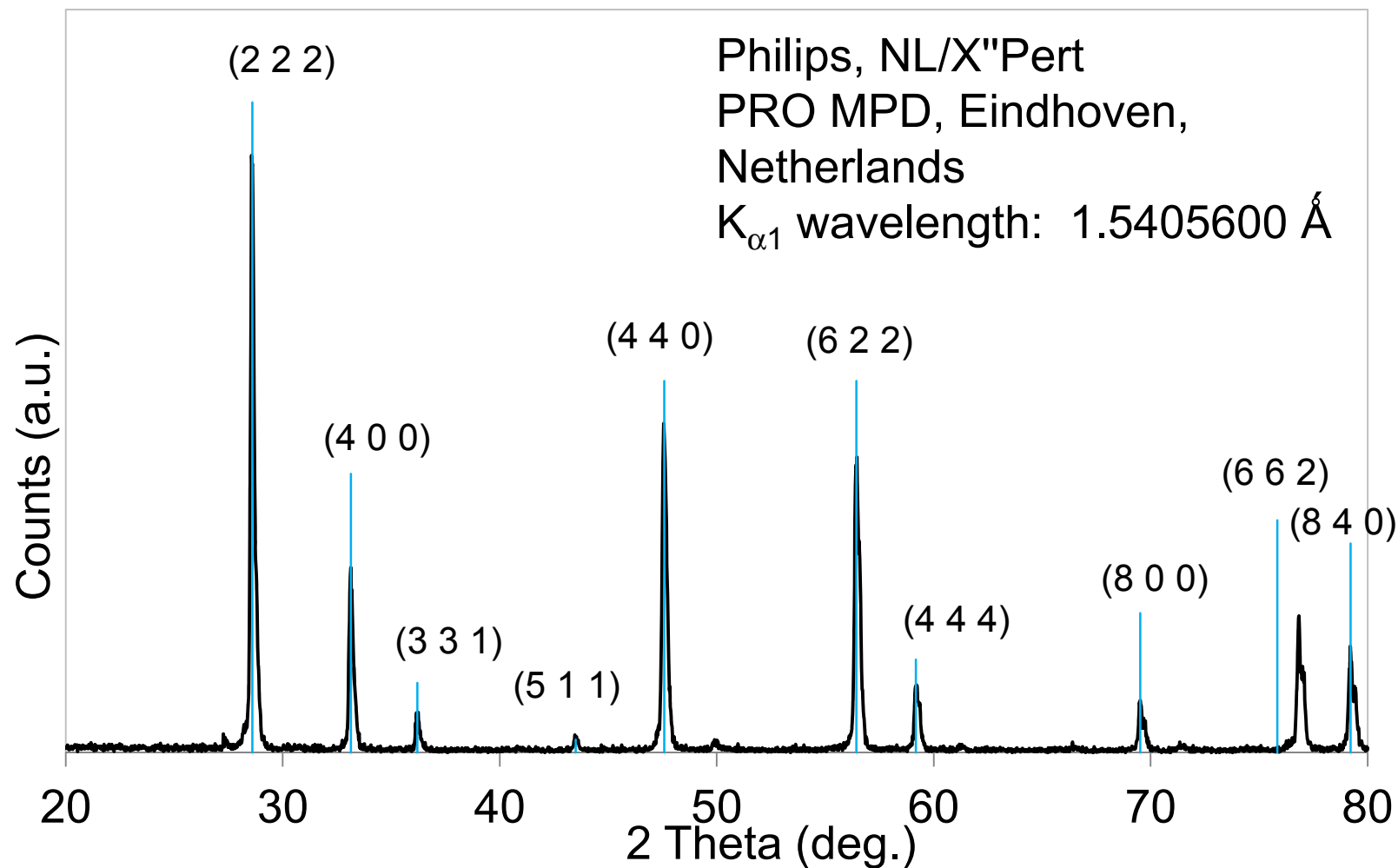
- Porous interior

TEM image of $\text{La}_2\text{Zr}_2\text{O}_7$



credit: Bin Hu @ Dartmouth

$\text{La}_2\text{Zr}_2\text{O}_7$ powder XRD analysis

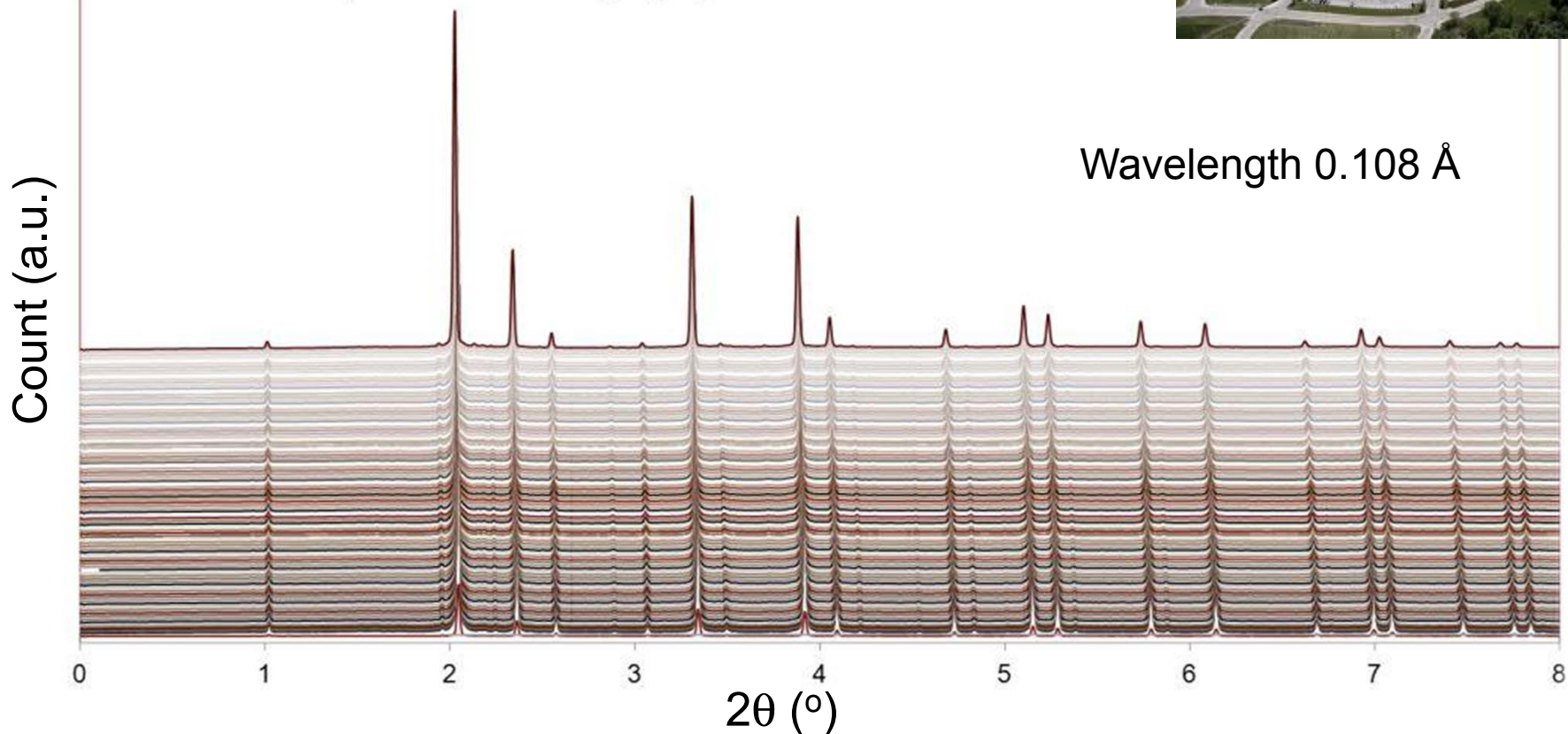


XRD data show that the powder composition is $\text{La}_2\text{Zr}_2\text{O}_7$

Synchrotron XRD



In situ HEXRD profiles of $\text{La}_2\text{Zr}_2\text{O}_7$ from 30°C to 1400°C



in situ synchrotron XRD shows no compositional change from 30 – 1400 °C.

credit: Yang Ren @ ANL

Coating fabrication using APS

- $\text{La}_2\text{Zr}_2\text{O}_7$ coatings were deposited using air plasma spray (APS) technique by a Praxair patented plasma spray torch.
- Haynes 188 superalloy was used as the substrate.

Haynes 188	Co	Ni	Cr	W	Si	C	La	Fe	Mn
(w%)	39	22	22	14	0.35	0.10	0.03	3	1.25

- The bond coat is Ni-based intermetallic LN-65 using APS, with a thickness of 228 μm

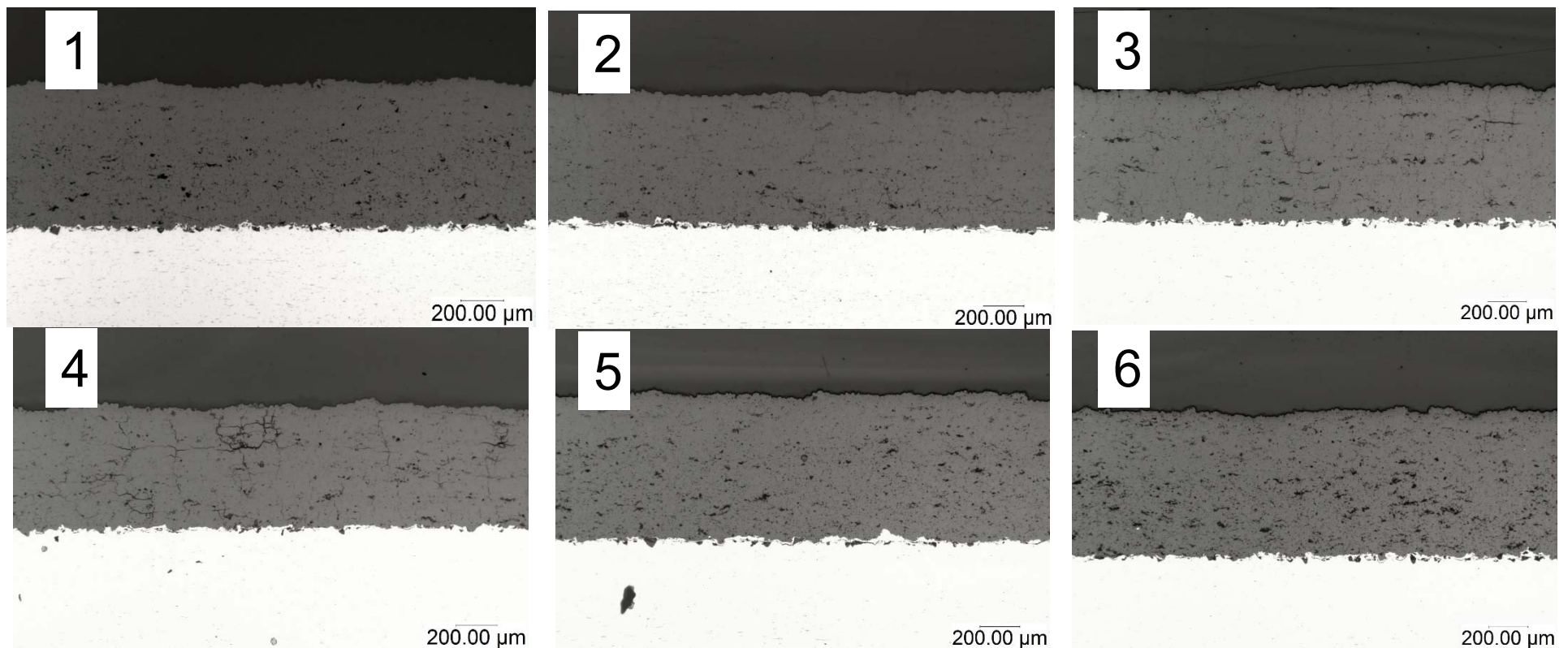
LN-65	Ni	Cr	Al	Y	O
(w%)	67.3	21.12	9.94	1.02	0.19

- Controlled spray parameters:
 - Powder feed ratio
 - Torch current
 - Torch gas (Argon), Carrier gas (Argon), Shield gas (Argon), Secondary gas (Hydrogen)
 - Standoff distance
 - Sample rig surface rotation speed (RPM and surface speed)

Outline

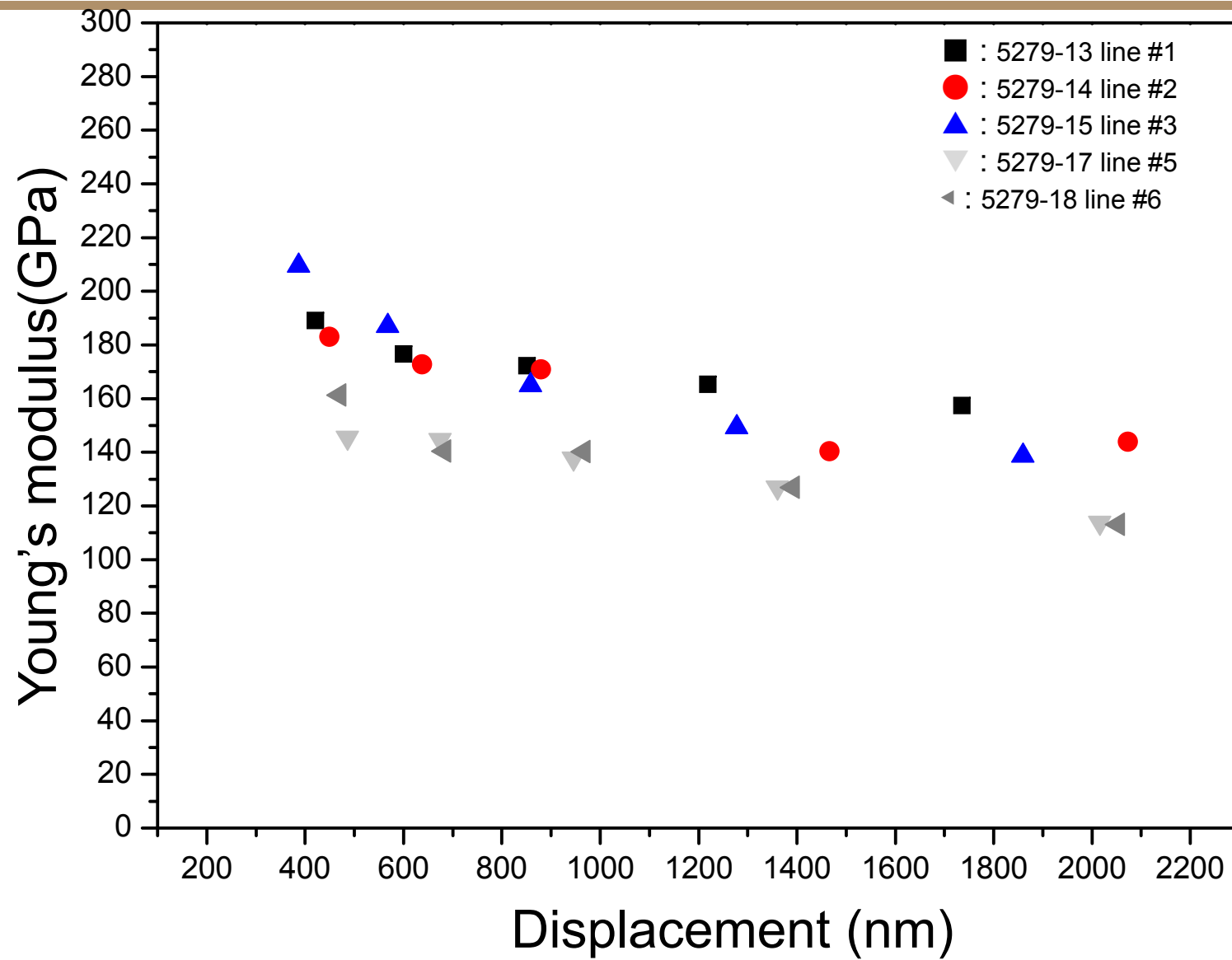
- Introduction
- **Coating design and fabrication**
 - **Single ceramic layer (SCL) – Dense Coat**
 - Composite coatings with buffer layers
- **Characterization of physical and mechanical properties**
 - **Microstructure and composition**
 - **Porosity and hardness**
 - Bond strength test
 - Erosion test
- Characterization of thermal property and thermal durability
 - Thermal conductivity, specific heat, coeff. of thermal expansion
 - Thermal shock (TS) test
 - Jet engine thermal shock (JETS) test
 - Furnace cycling thermal fatigue (FCTF) test
 - Thermal gradient mechanical fatigue (TGMF) test
- MD&FE modeling of thermal conductivity; DFT calculation of gas adsorption
- Summary and future work

Cross sectional view of dense coating

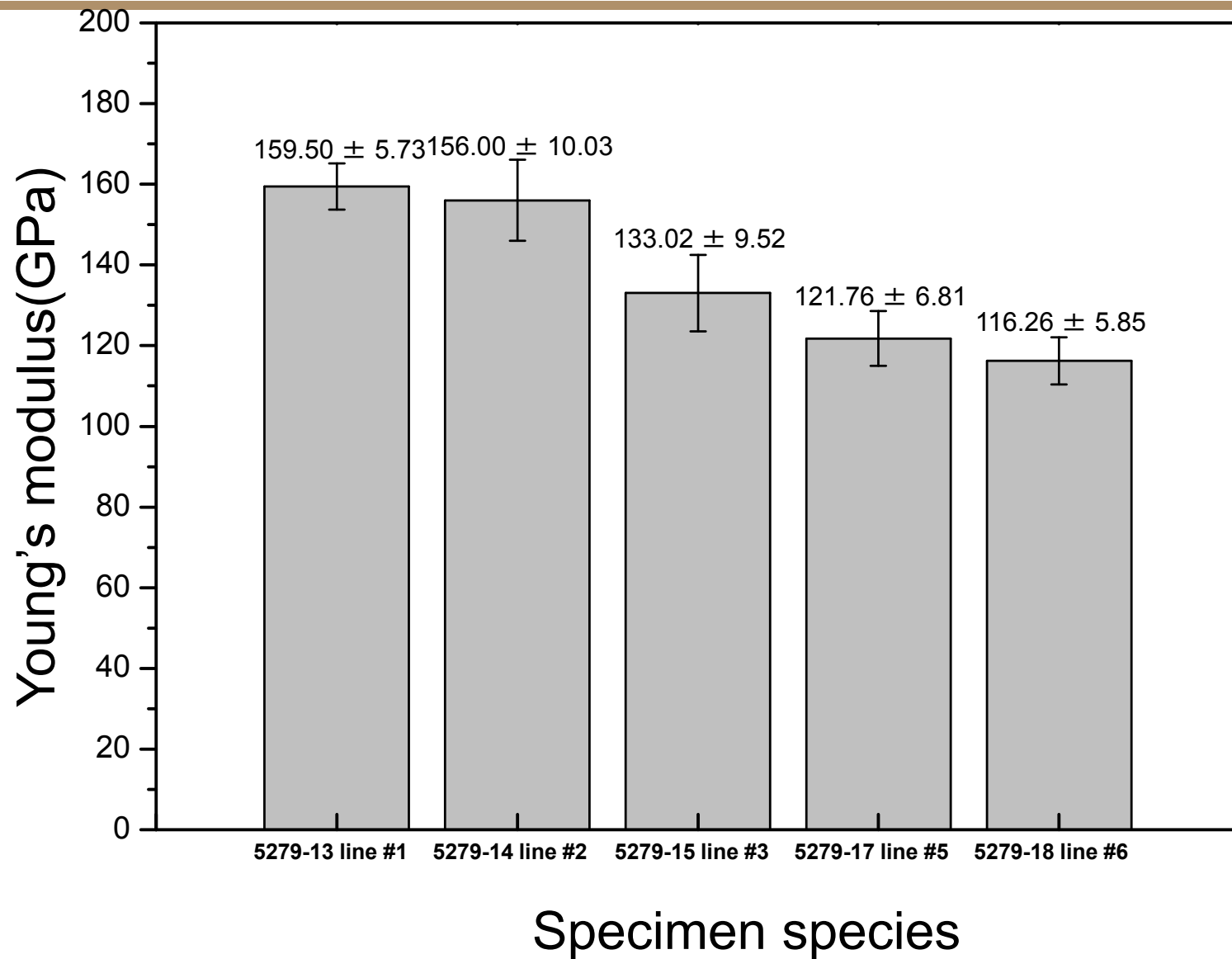


Processing parameters (powder feeding rate, surface speed, current, stand off) were varied to control the porosity.

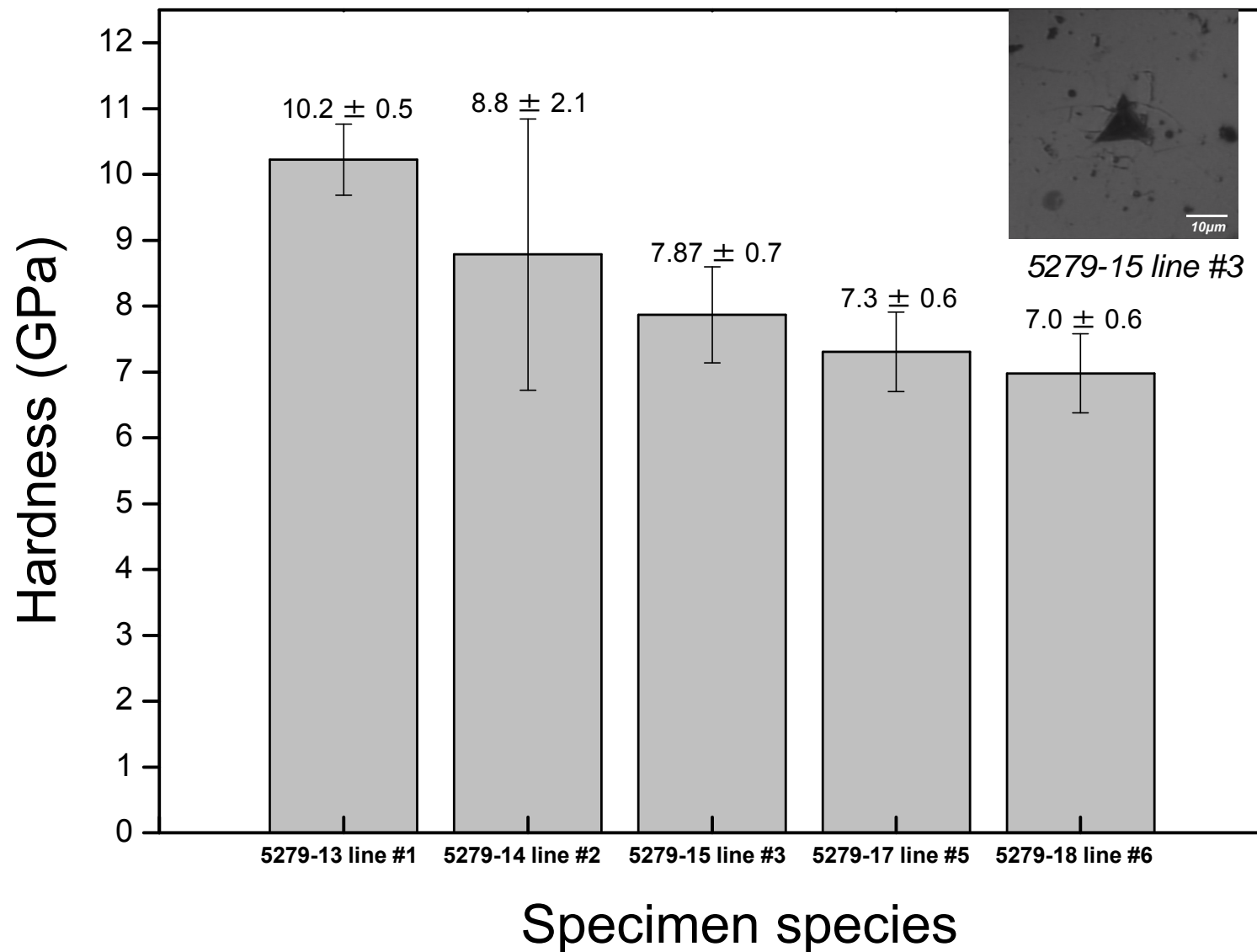
Nanoindentation Young's modulus vs. displacement



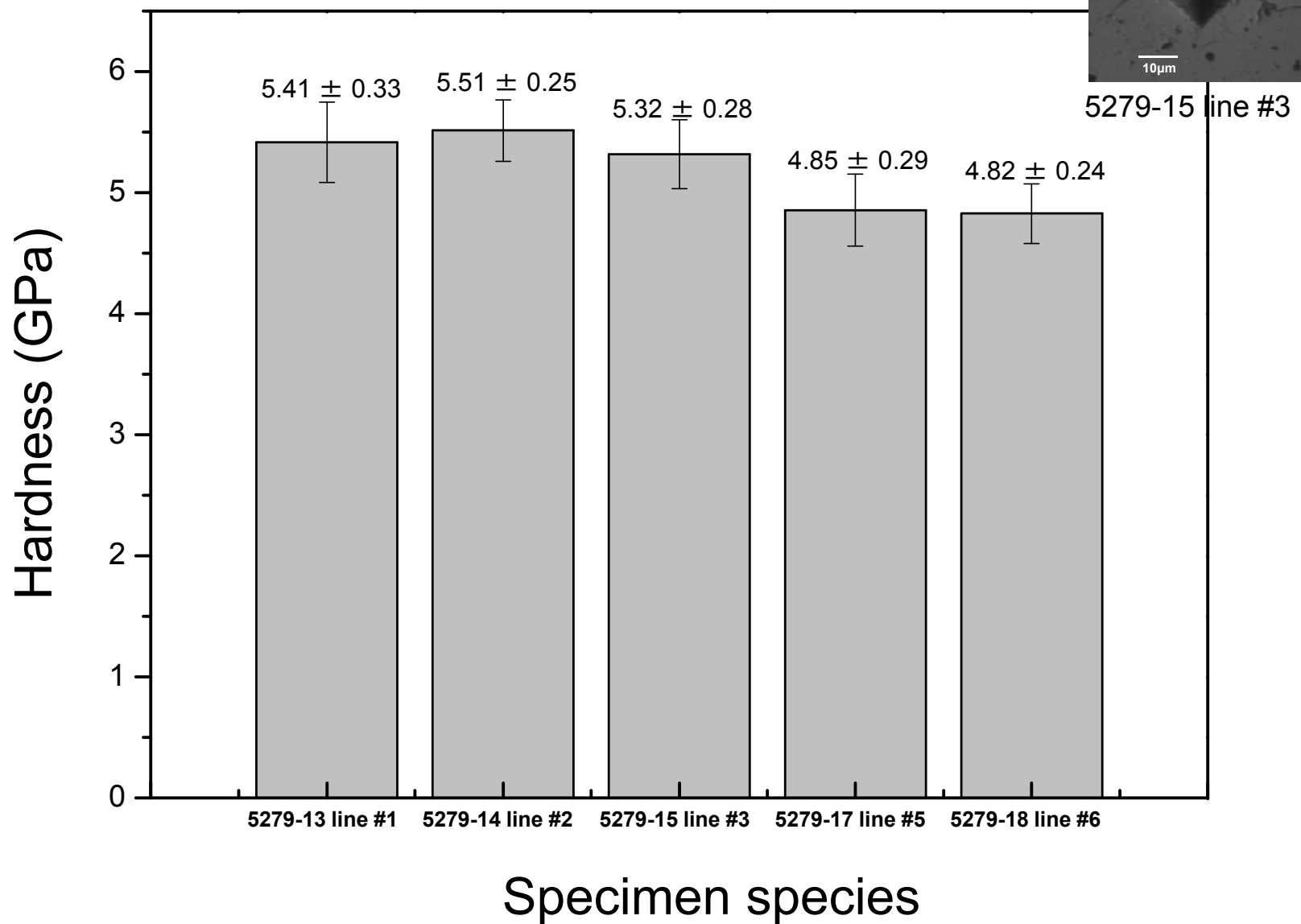
Nanoindentation Young's modulus



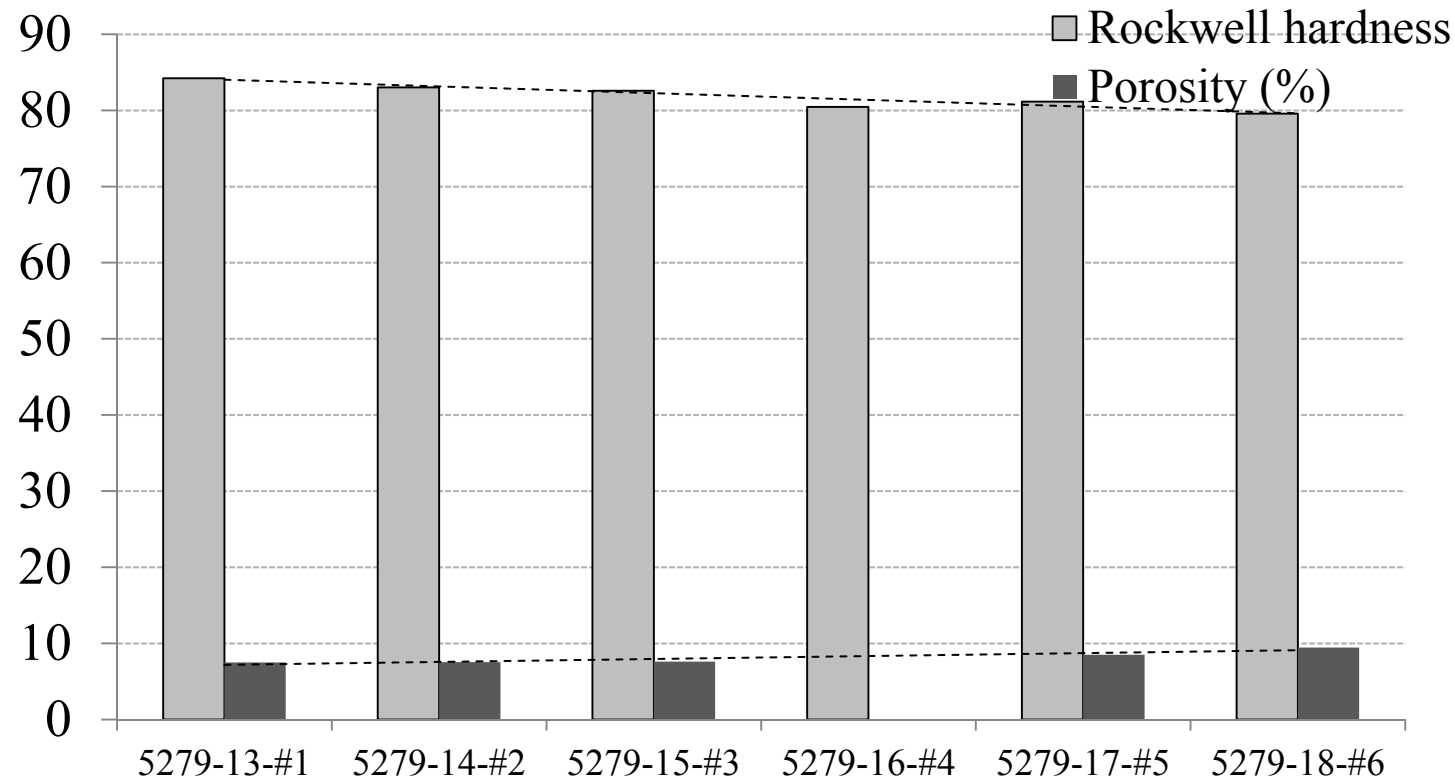
Nanoindentation hardness



Vicker's indentation hardness



Rockwell's indentation hardness

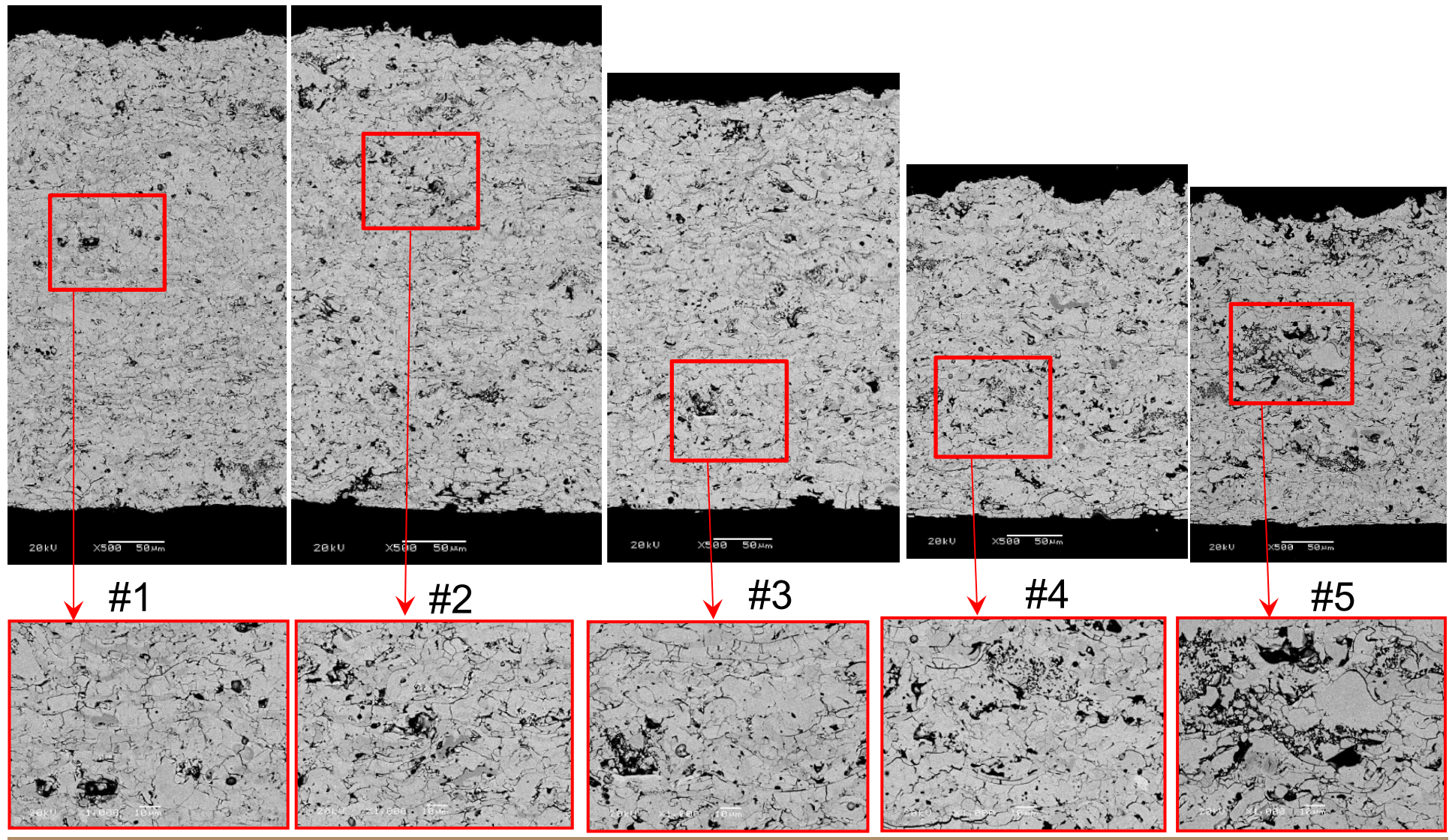


- Low density coatings with porosity between 7~10 % were achieved.
- Porosity and hardness can be tuned via changing processing conditions
- Powder feed rate↑ or current↓ → porosity↑ → hardness↓
[Hardness = $1.99 \times (100 - \text{porosity}) - 100$]

Outline

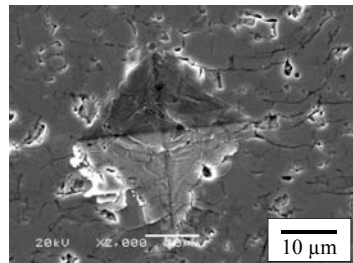
- Introduction
- **Coating design and fabrication**
 - **Single ceramic layer (SCL) – Porous Coat**
 - Composite coatings with buffer layers
- **Characterization of physical and mechanical properties**
 - **Microstructure and composition**
 - **Porosity and hardness**
 - Bond strength test
 - Erosion test
- Characterization of thermal property and thermal durability
 - Thermal conductivity, specific heat, coeff. of thermal expansion
 - Thermal shock (TS) test
 - Jet engine thermal shock (JETS) test
 - Furnace cycling thermal fatigue (FCTF) test
 - Thermal gradient mechanical fatigue (TGMF) test
- MD&FE modeling of thermal conductivity; DFT calculation of gas adsorption
- Summary and future work

Cross sections of SCL $\text{La}_2\text{Zr}_2\text{O}_7$ coatings

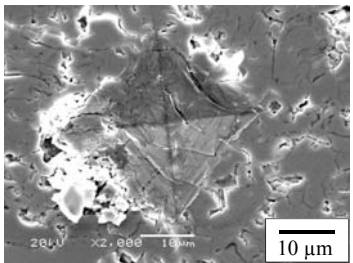


Vickers hardness indentation

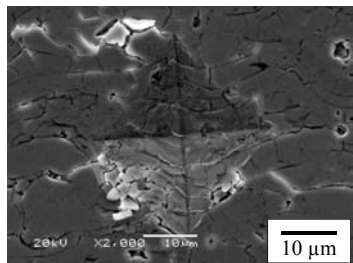
#1



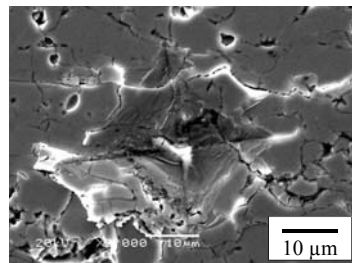
#2



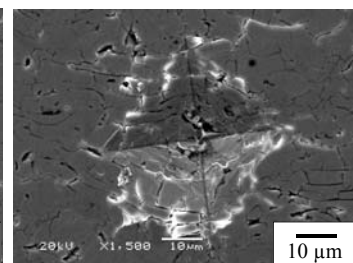
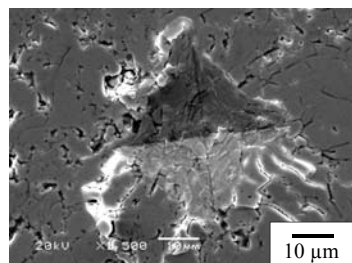
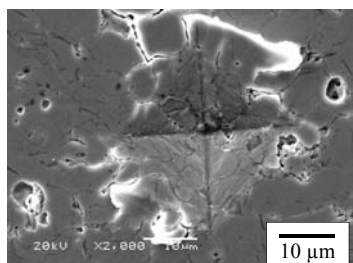
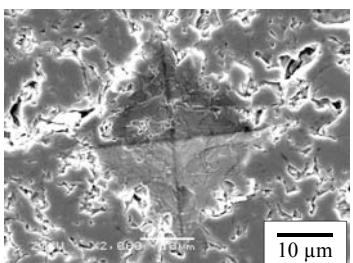
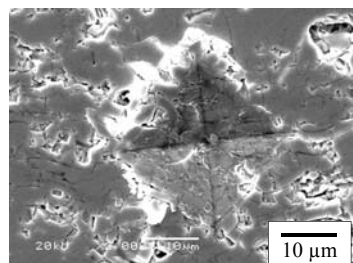
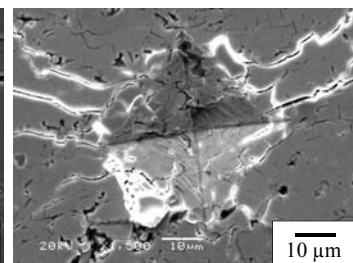
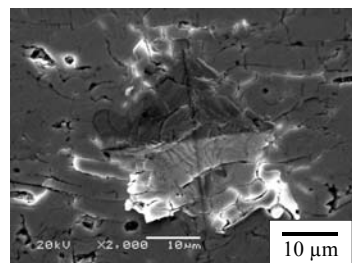
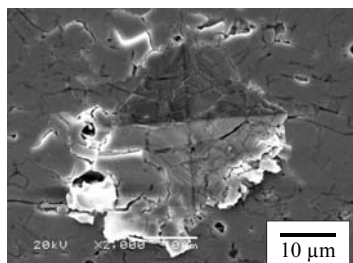
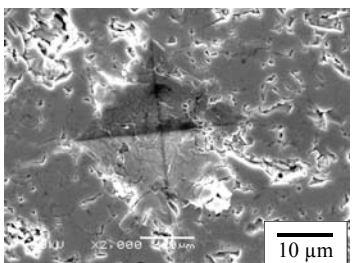
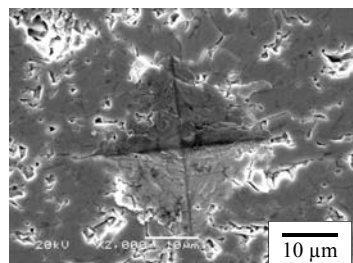
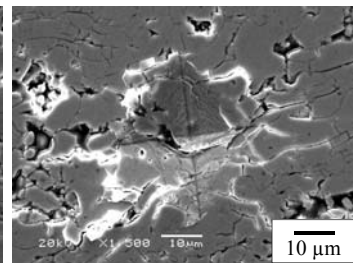
#3



#4

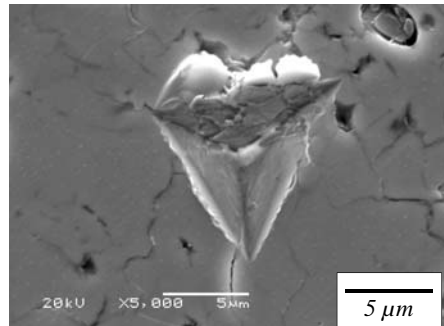


#5

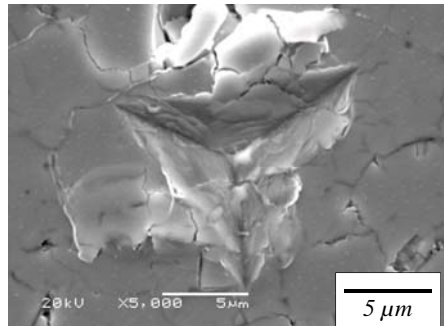


Nanoindentation

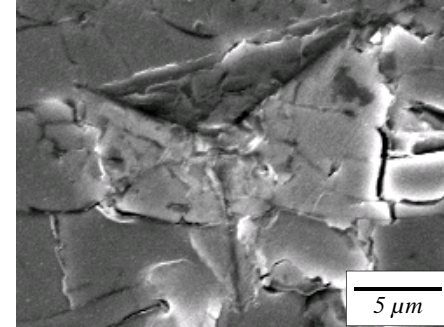
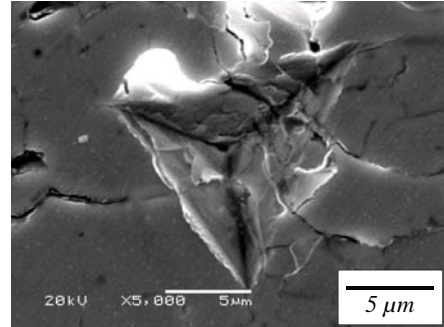
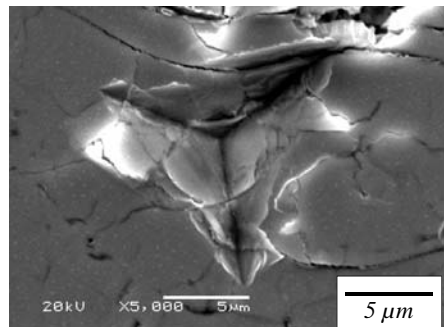
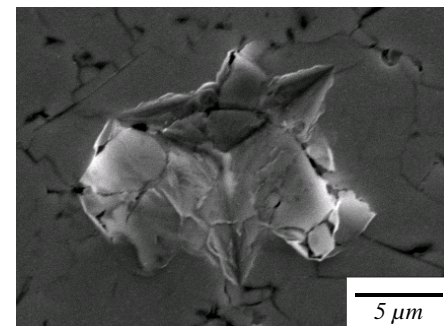
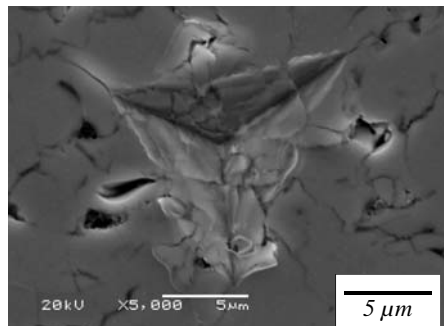
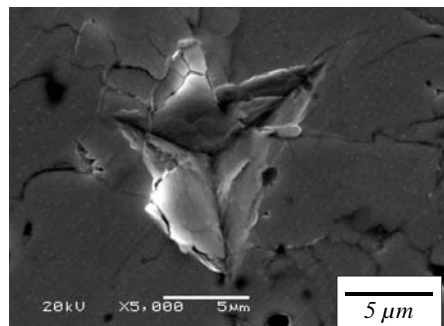
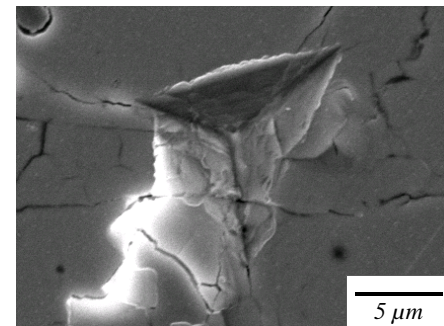
#3



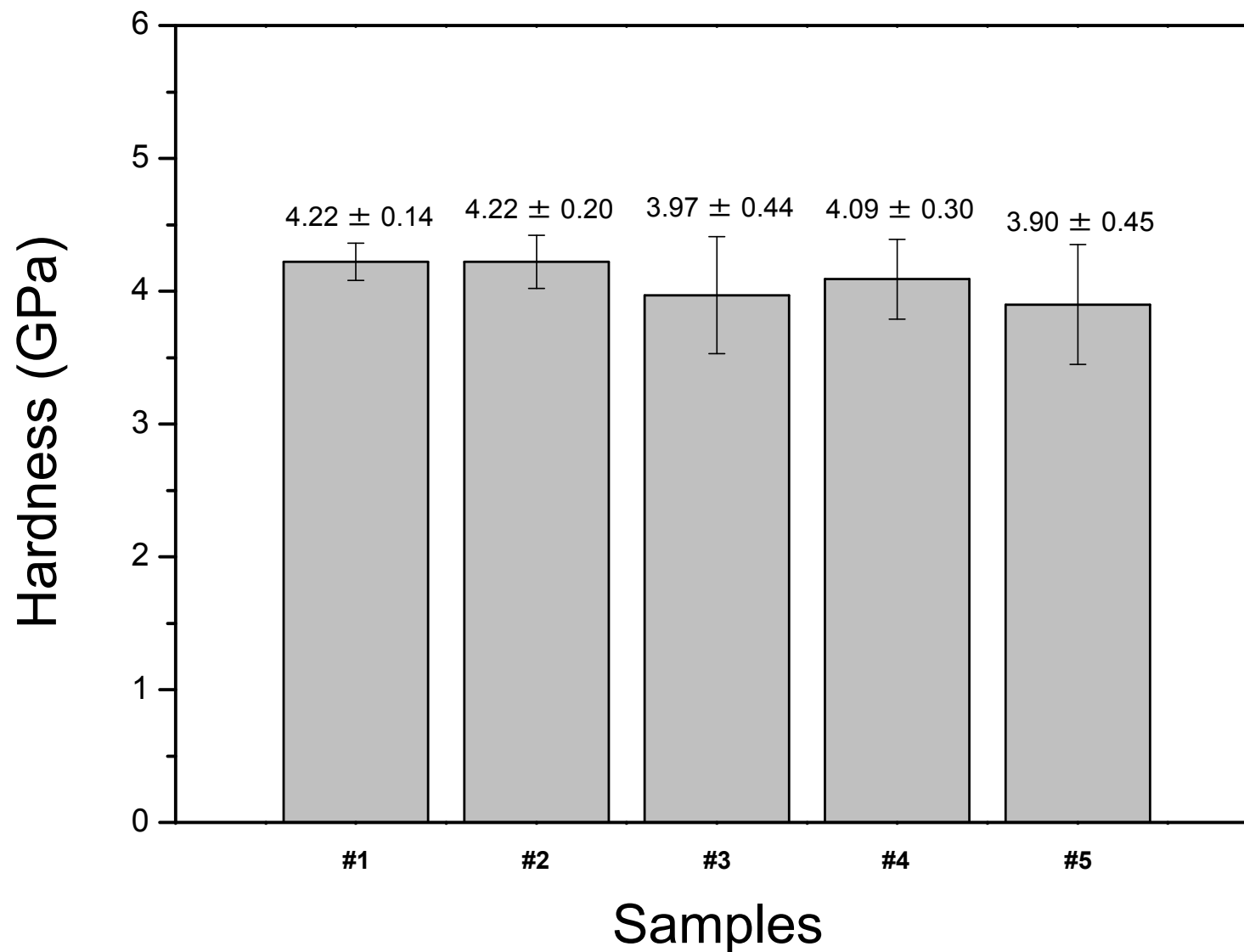
#4



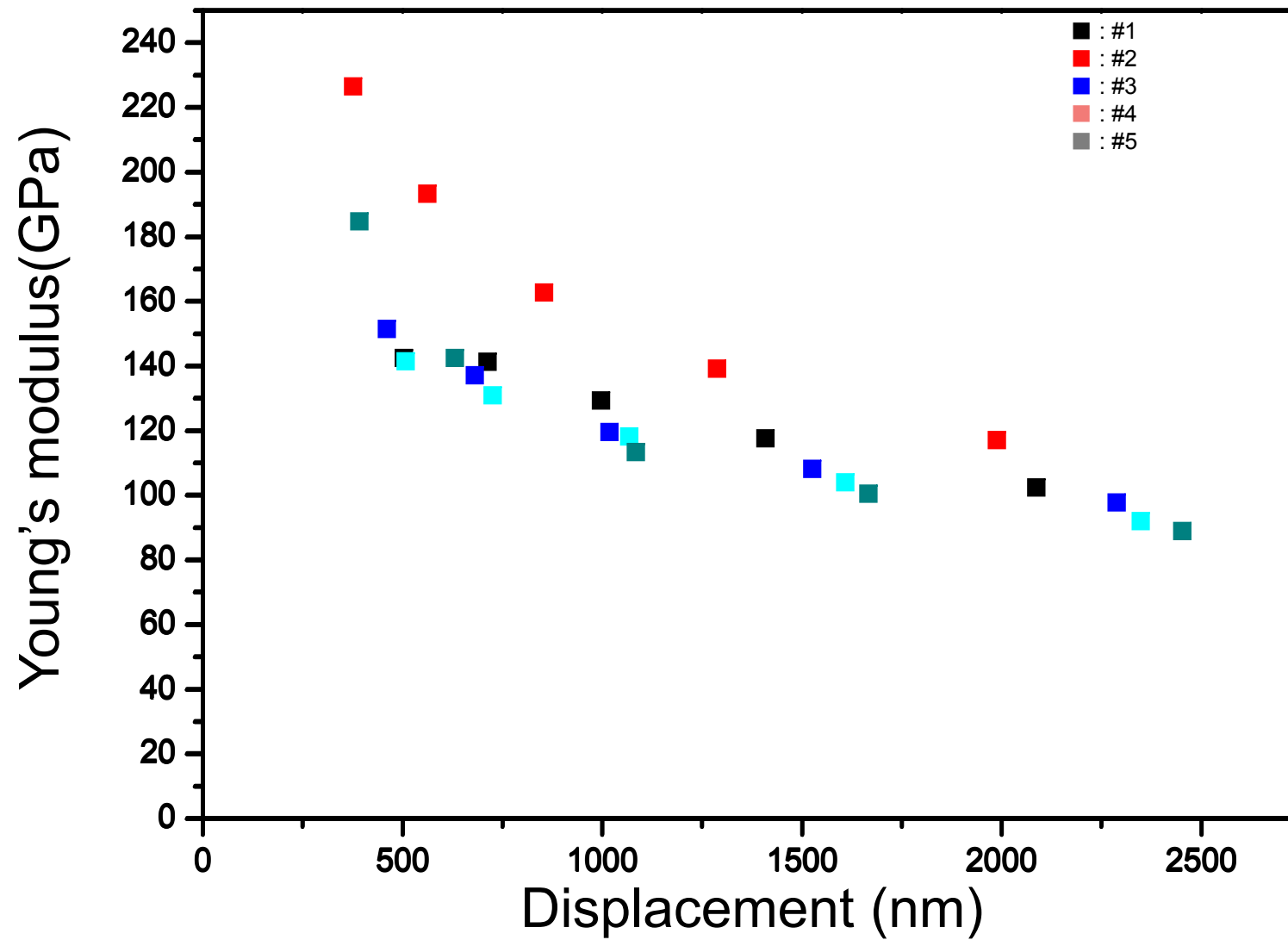
#5



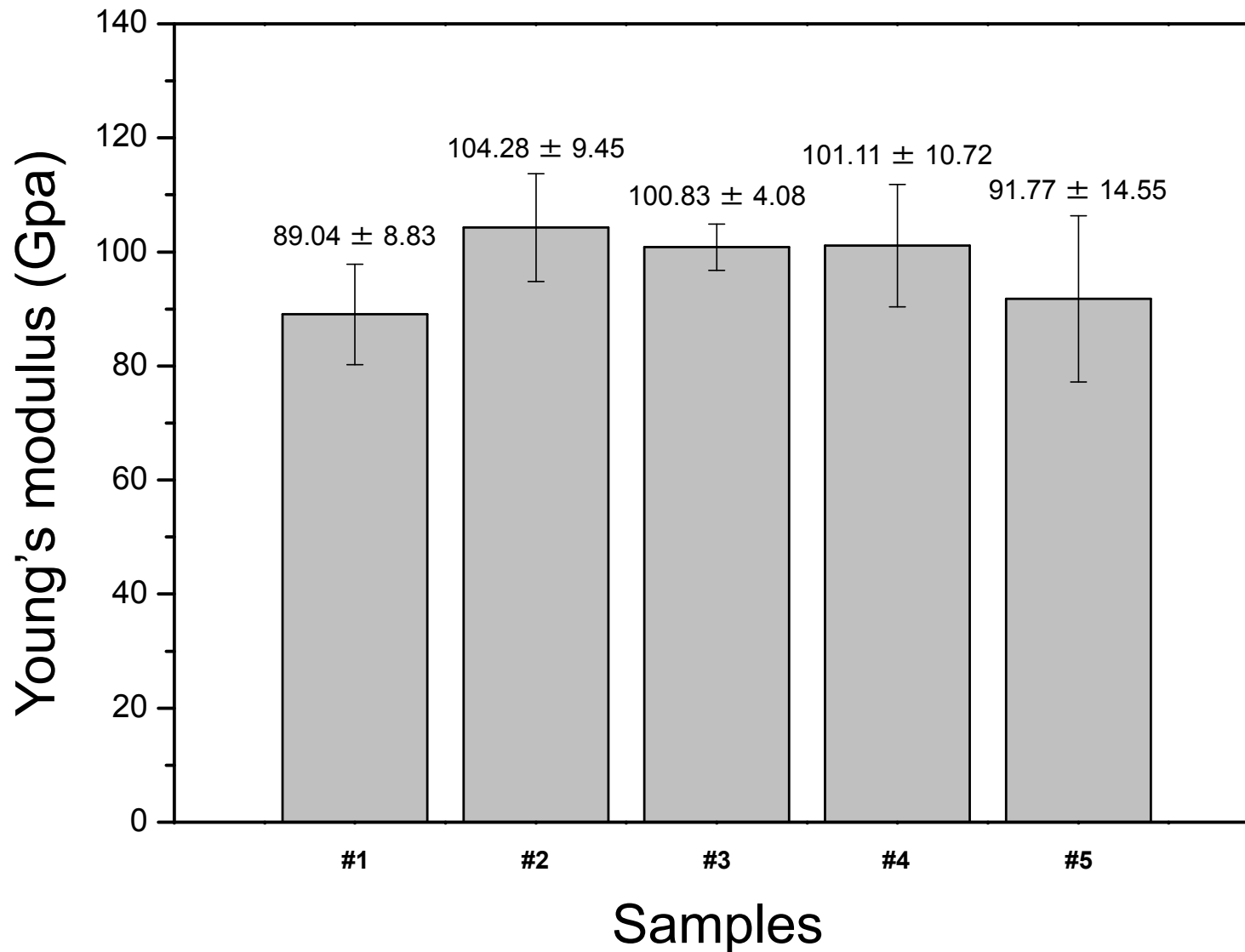
Vickers indentation hardness



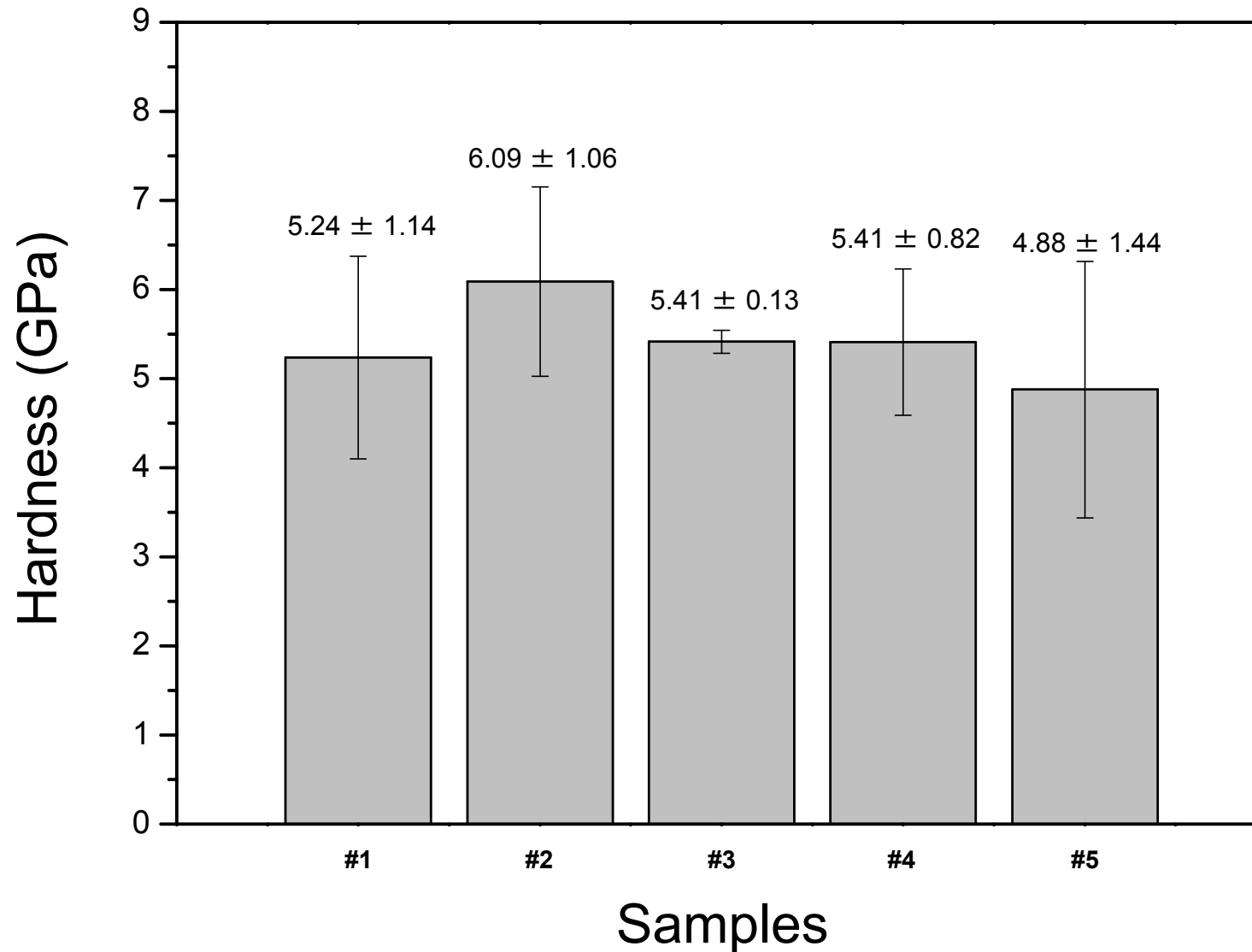
Nano indentation Young's modulus vs. displacement



Nanoindentation Young's modulus



Nanoindentation hardness



Porosity of low density SCL coating

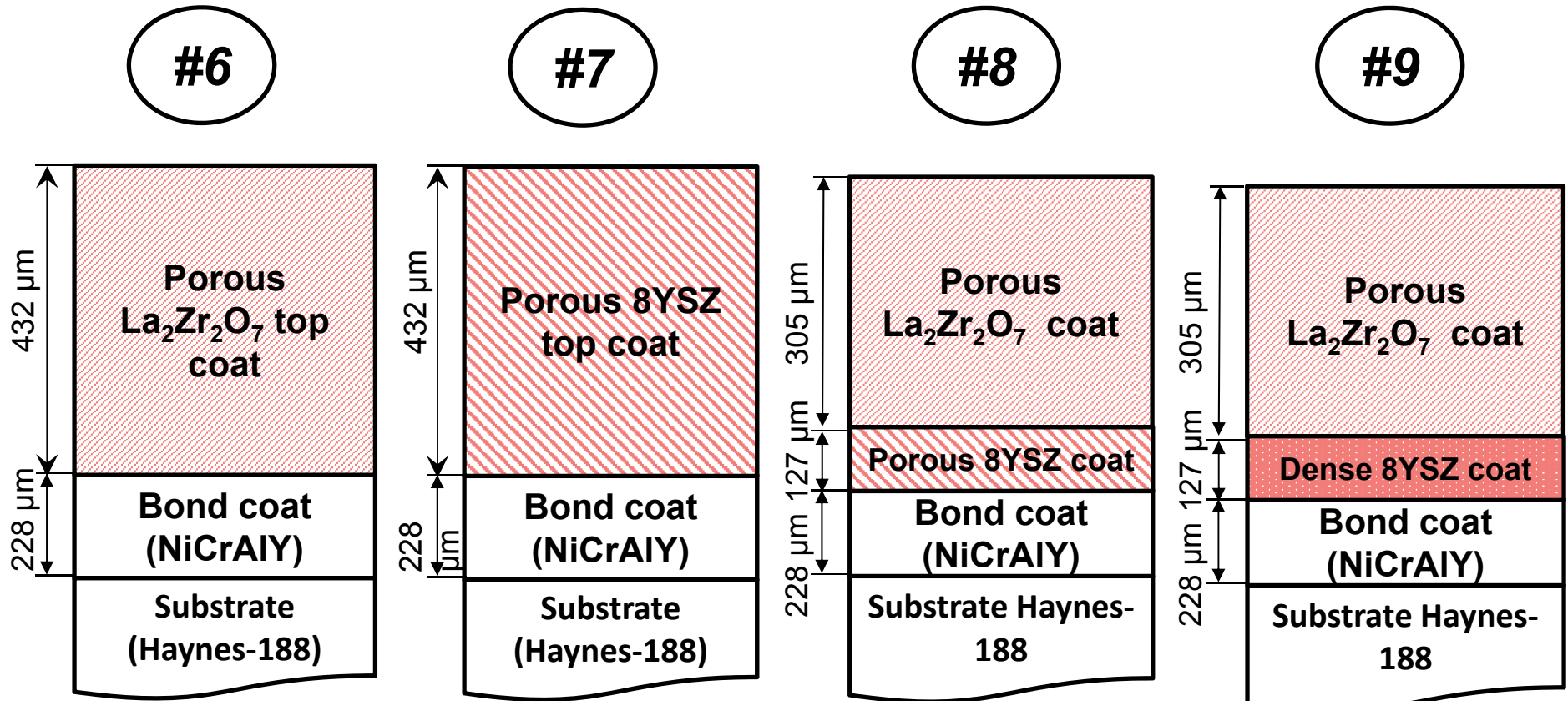
Line #	Density (g/cm ³)	Porosity (%)
7	5.3182	11.36
8	5.2587	12.36
9	5.2584	12.36
10	5.2917	11.81
11	5.2614	12.31
12	5.0089	16.52

Low density coatings with porosity between 11~17% were achieved.

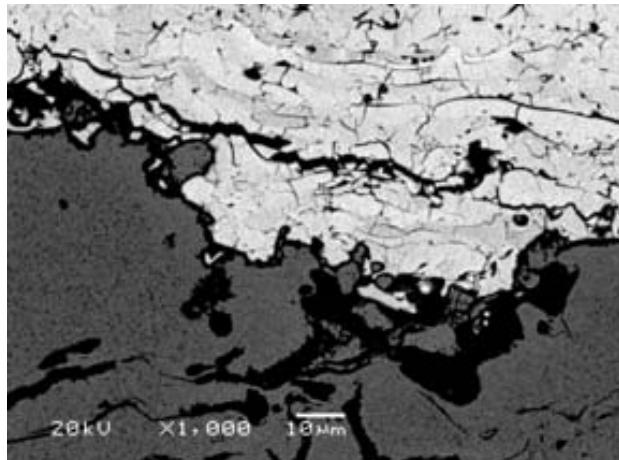
Outline

- Introduction
- **Coating design and fabrication**
 - **Double ceramic layer (DCL) coats**
 - Composite coatings with buffer layers
- **Characterization of physical and mechanical properties**
 - **Microstructure and composition**
 - **Porosity and hardness**
 - Bond strength test
 - Erosion test
- Characterization of thermal property and thermal durability
 - Thermal conductivity, specific heat, coeff. of thermal expansion
 - Thermal shock (TS) test
 - Jet engine thermal shock (JETS) test
 - Furnace cycling thermal fatigue (FCTF) test
 - Thermal gradient mechanical fatigue (TGMF) test
- MD&FE modeling of thermal conductivity; DFT calculation of gas adsorption
- Summary and future work

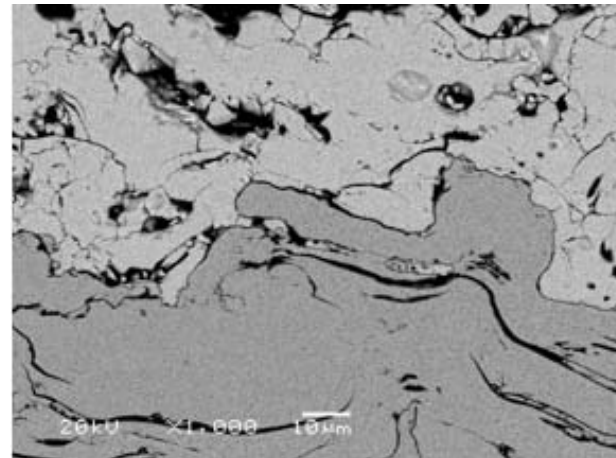
Double ceramic layer (DCL) architectures



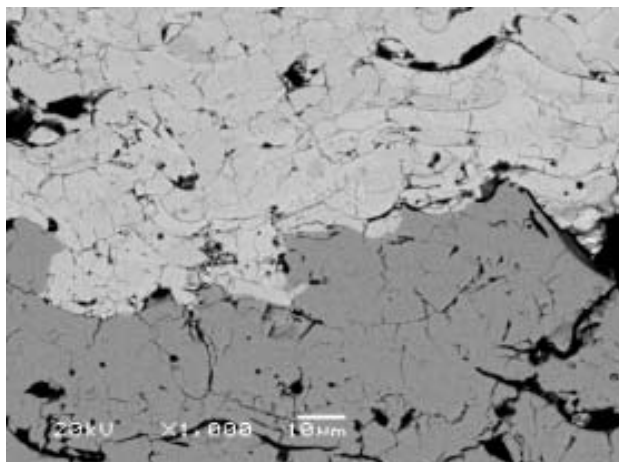
Interfaces of DCL coatings



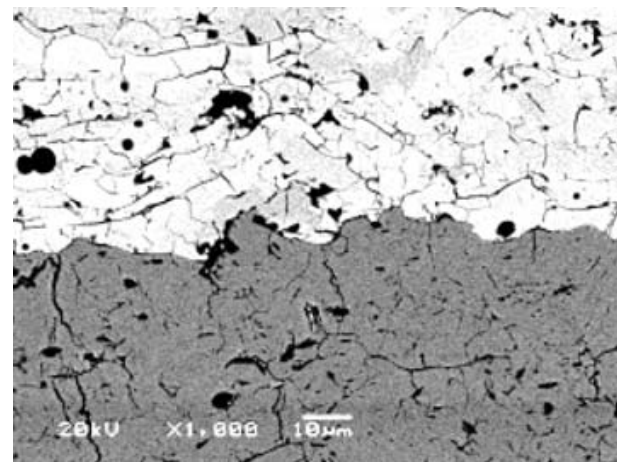
#6 La₂Zr₂O₇ and bond coat interface



#7 porous 8YSZ and bond coat interface



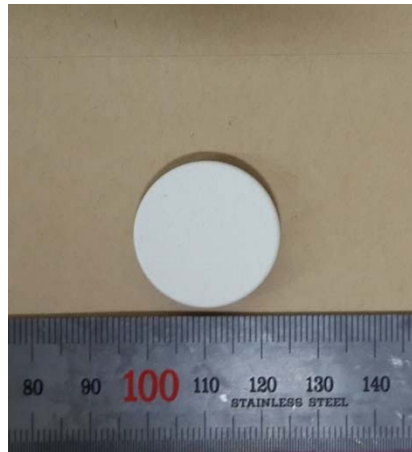
#8 La₂Zr₂O₇ and porous 8YSZ interface



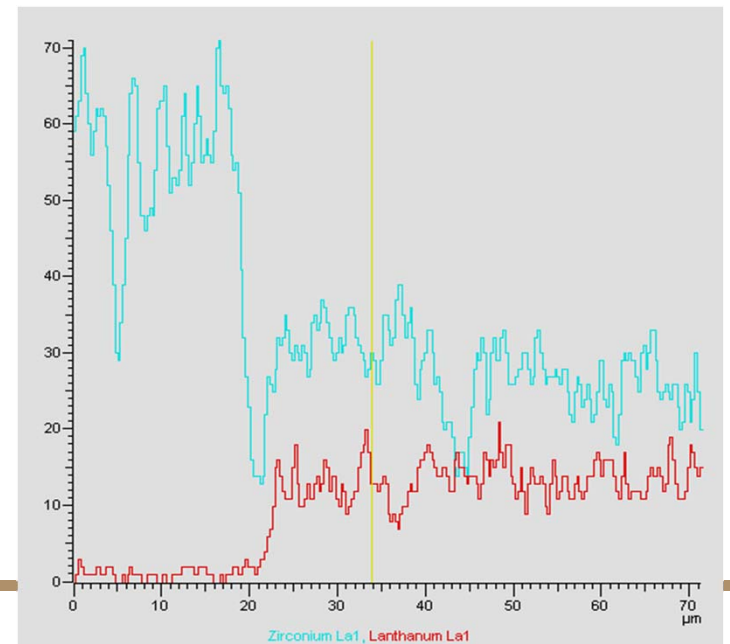
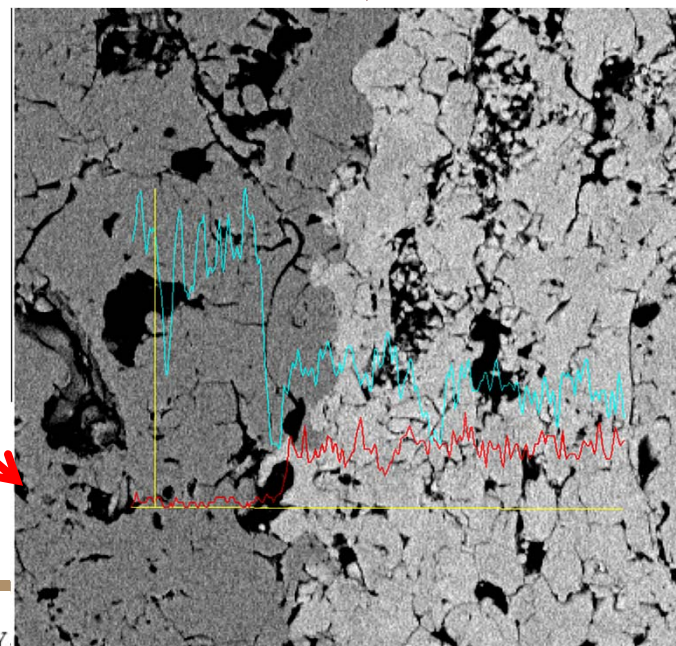
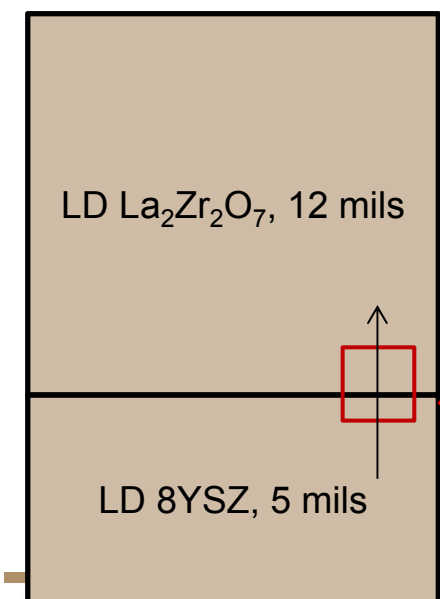
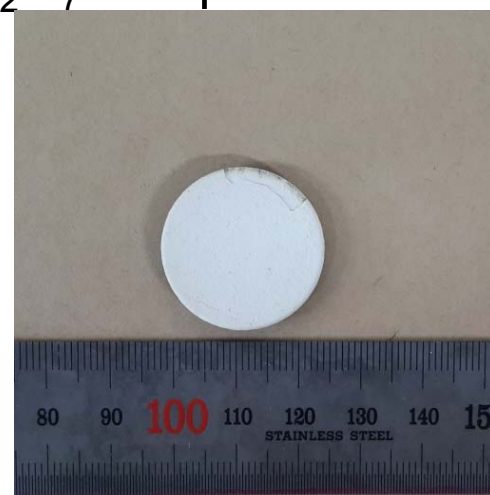
#9 La₂Zr₂O₇ and dense 8YSZ interface

Energy-dispersive X-ray spectroscopy

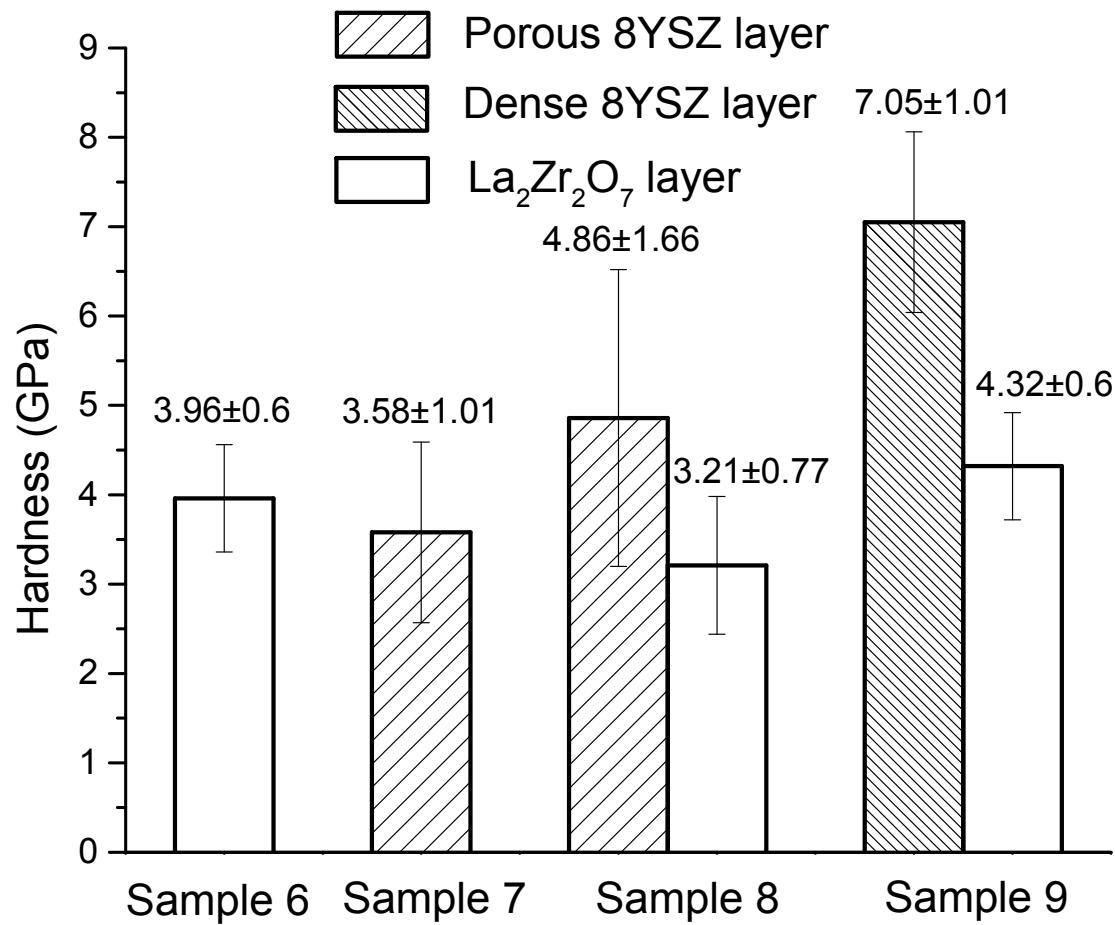
Applied heat treatments on sample #8: 8 La₂Zr₂O₇ and porous 8YSZ



Heat treatment
1080°C 4h
Ar atmosphere



Vickers hardness of DCL coatings

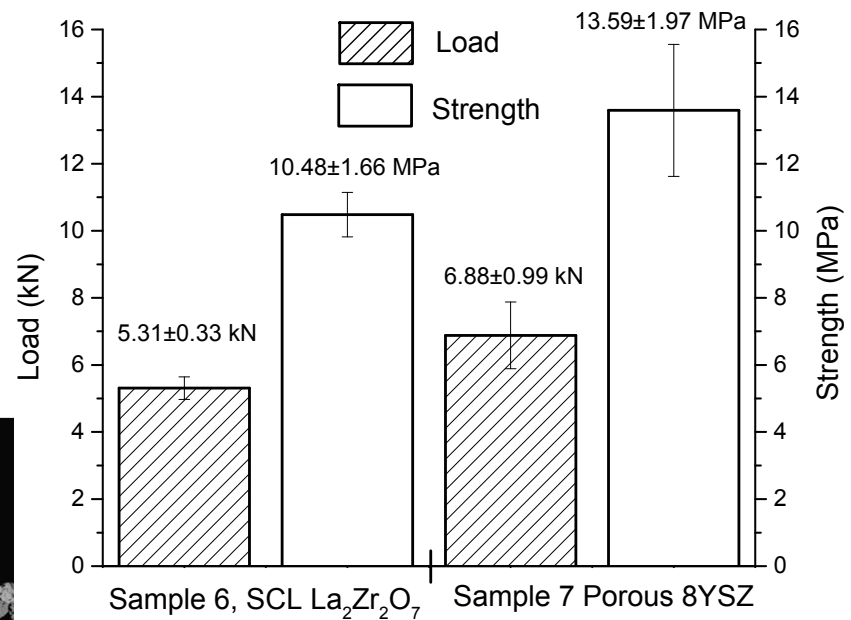
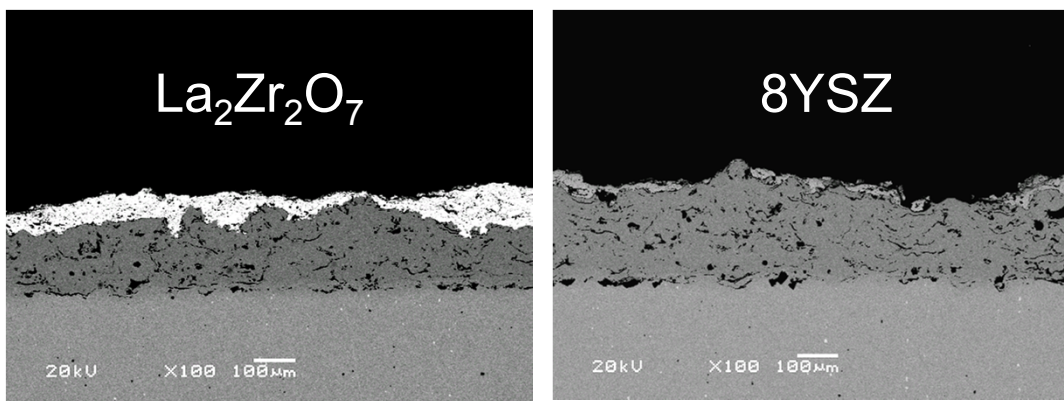
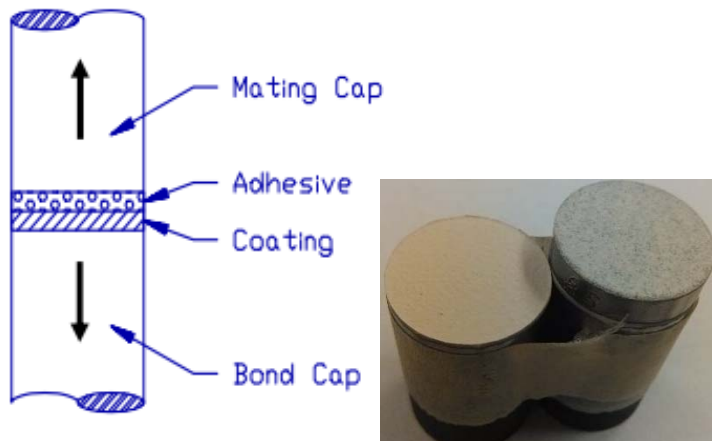


Outline

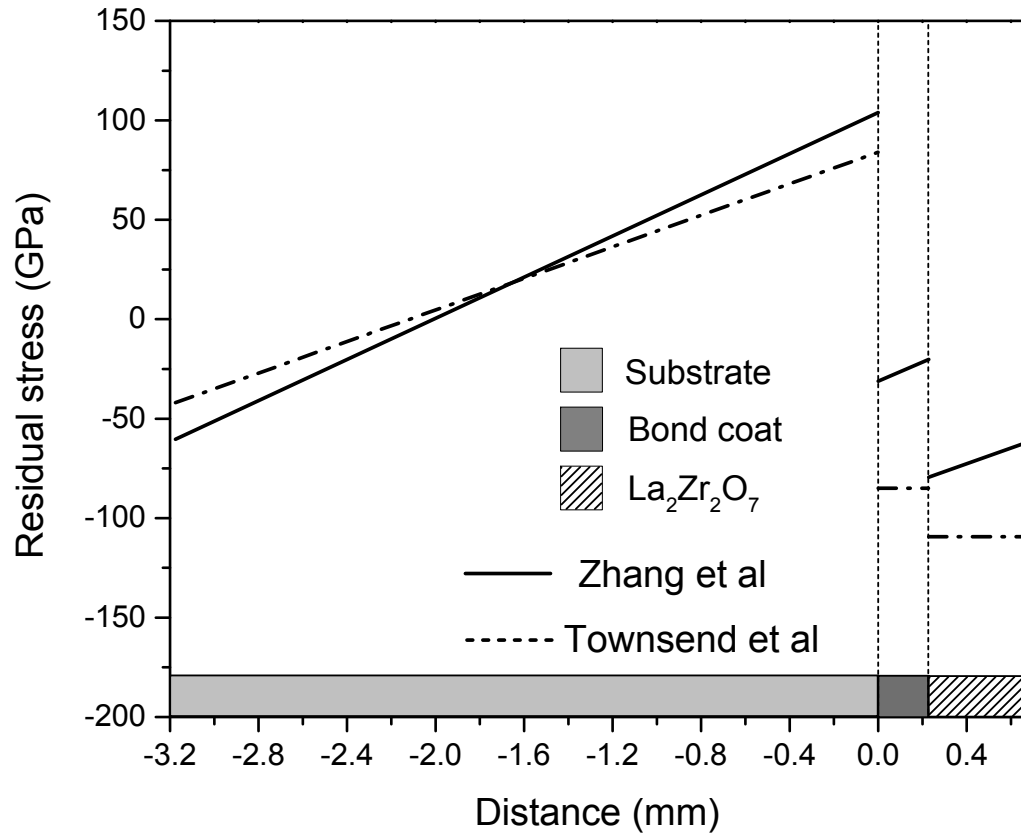
- Introduction
- Coating design and fabrication
 - Single ceramic layer (SCL) & Double ceramic layer (DCL) architectures
 - Composite coatings with buffer layers
- **Characterization of physical and mechanical properties**
 - Microstructure and composition
 - Porosity and hardness
 - **Bond strength test**
 - **Erosion test**
- Characterization of thermal property and thermal durability
 - Thermal conductivity, specific heat, coeff. of thermal expansion
 - Thermal shock (TS) test
 - Jet engine thermal shock (JETS) test
 - Furnace cycling thermal fatigue (FCTF) test
 - Thermal gradient mechanical fatigue (TGMF) test
- MD&FE modeling of thermal conductivity; DFT calculation of gas adsorption
- Summary and future work

Bond strength test

Epoxy (FM 1000 adhesive film) to glue coating buttons to a mating cap.
Tensile test according to ASTM-C-633.



Residual stress distribution in coating



$$\sigma_s = E_s \left[\varepsilon_s + K(z + \delta) \right]$$

$$\sigma_i = E_i \left[\varepsilon_i + K(z + \delta) \right]$$

where $\varepsilon_i = \Delta\alpha\Delta T + \sum_{k=1}^n \frac{E_k t_k}{E_s t_s} (\alpha_k - \alpha_i) \Delta T$

$$\varepsilon_s = -\sum_{i=1}^n \frac{E_i t_i}{E_s t_s} \Delta\alpha\Delta T$$

$$\delta = \frac{t_s}{2} - \sum_{i=1}^n \frac{E_i t_i}{E_s t_s} (2h_{i-1} + t_i)$$

$$K = -\sum_{i=1}^n \frac{6E_i t_i \Delta\alpha\Delta T}{E_s t_s^2}$$

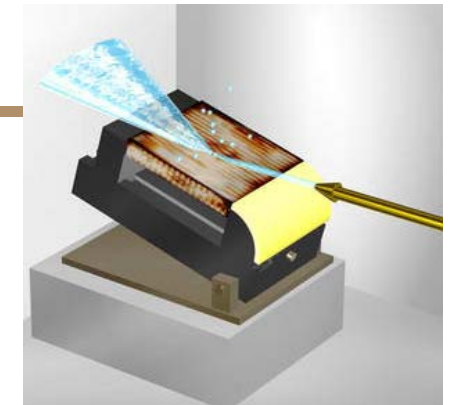
where α is the coefficient of thermal expansion (CTE), k is the ceramic coating layers range from 1 to n , t_i is the thickness of i^{th} layer.

X.C. Zhang, *Thin Solid Films*, 488 (2005) 274-282.

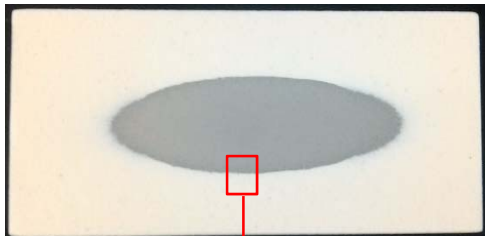
- Guo *et al.*, Thermal properties, thermal shock and thermal cycling behavior of lanthanum zirconate based thermal barrier coatings, *Metallurgical and Materials Transactions E*, (DOI: 10.1007/s40553-016-0070-4)

Erosion test

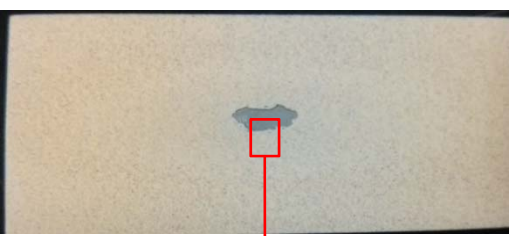
- $600 \pm 0.2\text{g}$ alumina sands with a diameter of $50\text{ }\mu\text{m}$
- Spray rate 6 g/s ; duration 100 s ; spray angle 20°



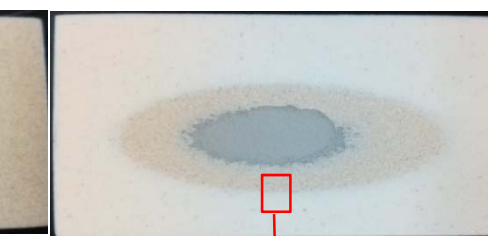
#6, Single layer $\text{La}_2\text{Zr}_2\text{O}_7$



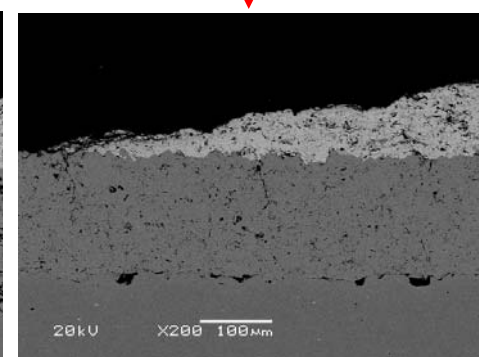
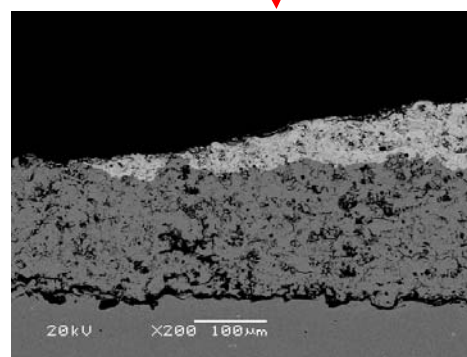
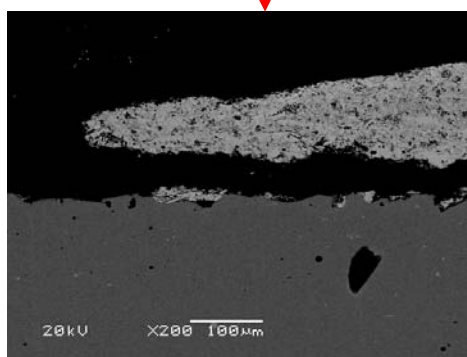
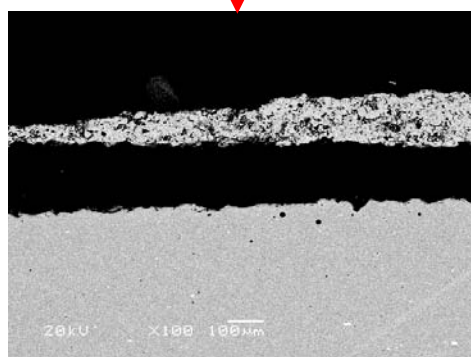
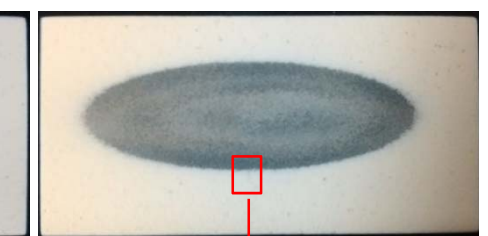
#7, Porous 8YSZ



#8, $\text{La}_2\text{Zr}_2\text{O}_7 +$ Porous 8YSZ



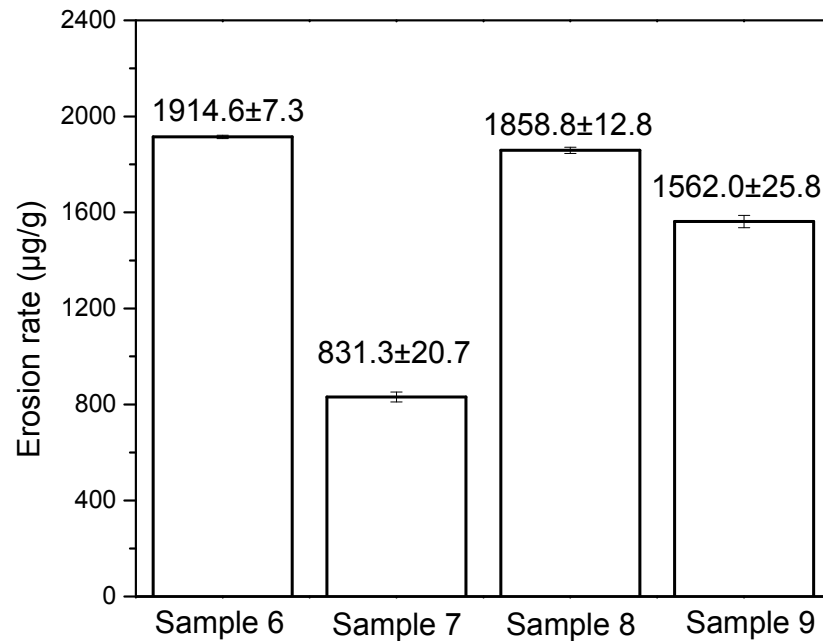
#9, $\text{La}_2\text{Zr}_2\text{O}_7 +$ Dense 8YSZ



Erosion rate & critical erosion velocity

Erosion rate describes the erosion resistance of TBC sample [1]:

$$R_{\text{erosion}} = \frac{W_{\text{removed material}}}{W_{\text{impacting particles}}}$$

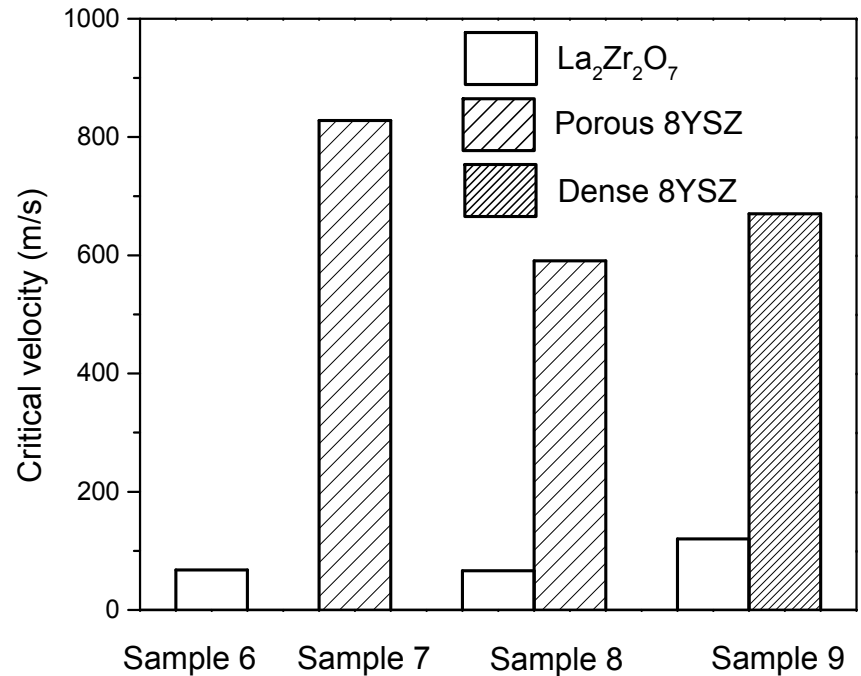


[1] D. Park, Int J Adv Manuf Technol, 23 (2004) 444-450.

Critical erosion velocity is used to express the critical condition to initiate cracks [2]:

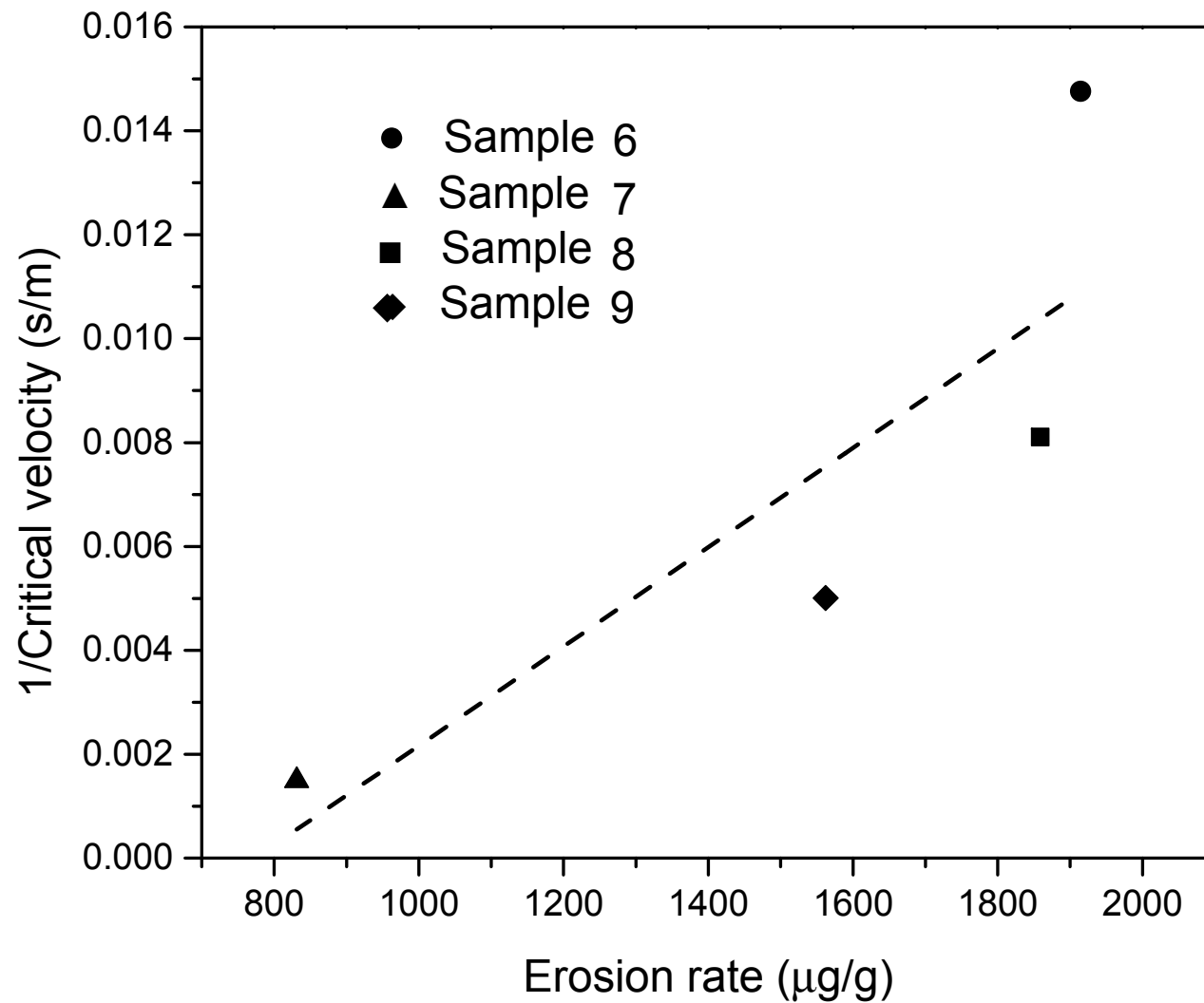
$$V_{\text{crit}} = 105 \frac{E^{3/4} K_{\text{IC}}^3}{H^{13/4} \rho^{1/2} R^{3/2}}$$

E: Young's modulus
H: hardness
 K_{IC} : fracture toughness
 ρ : density of erodent particle
R: particle radius



[2] R.G. Wellman, Wear, 256 (2004) 889-899.

Relationship between V_{crit} and erosion rate



Outline

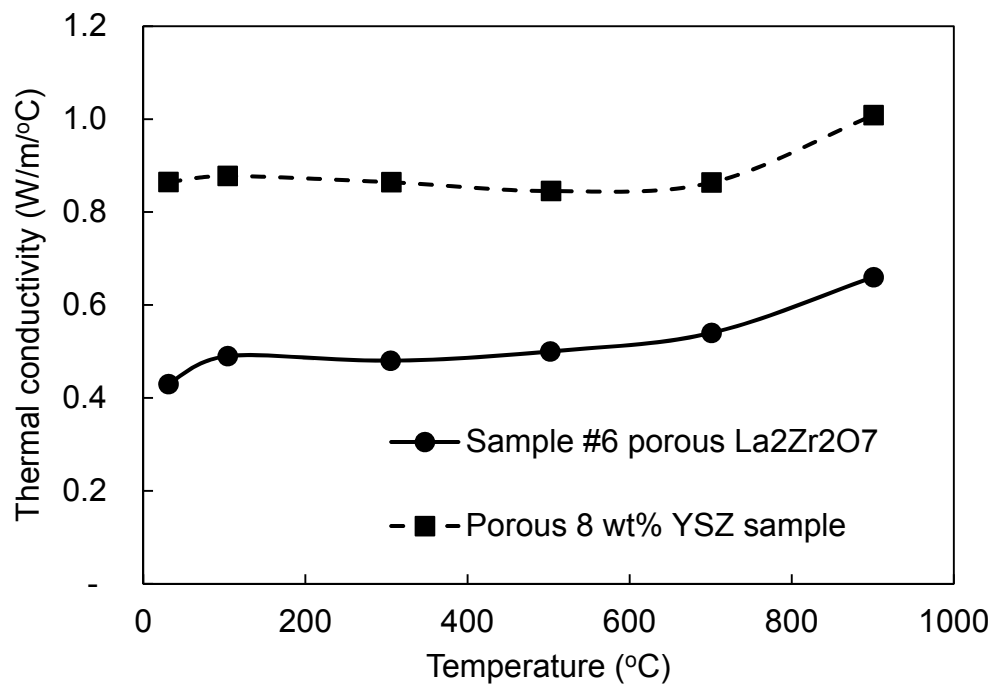
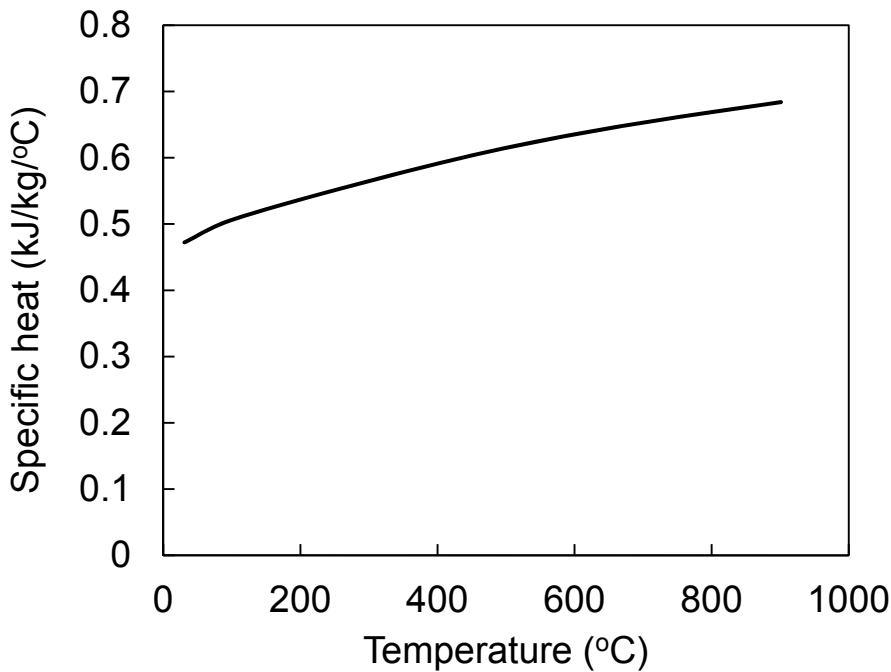
- Introduction
- Coating design and fabrication
 - Single ceramic layer (SCL) & Double ceramic layer (DCL) architectures
 - Composite coatings with buffer layers
- Characterization of physical and mechanical properties
 - Microstructure and composition
 - Porosity and hardness
 - Bond strength test
 - Erosion test
- **Characterization of thermal property** and thermal durability
 - **Thermal conductivity, specific heat, coeff. of thermal expansion**
 - Thermal shock (TS) test
 - Jet engine thermal shock (JETS) test
 - Furnace cycling thermal fatigue (FCTF) test
 - Thermal gradient mechanical fatigue (TGMF) test
- MD&FE modeling of thermal conductivity; DFT calculation of gas adsorption
- Summary and future work

Thermal conductivity

Thermal conductivity is determined from thermal diffusivity D_{th} , specific heat capacity C_p , and measured density ρ :

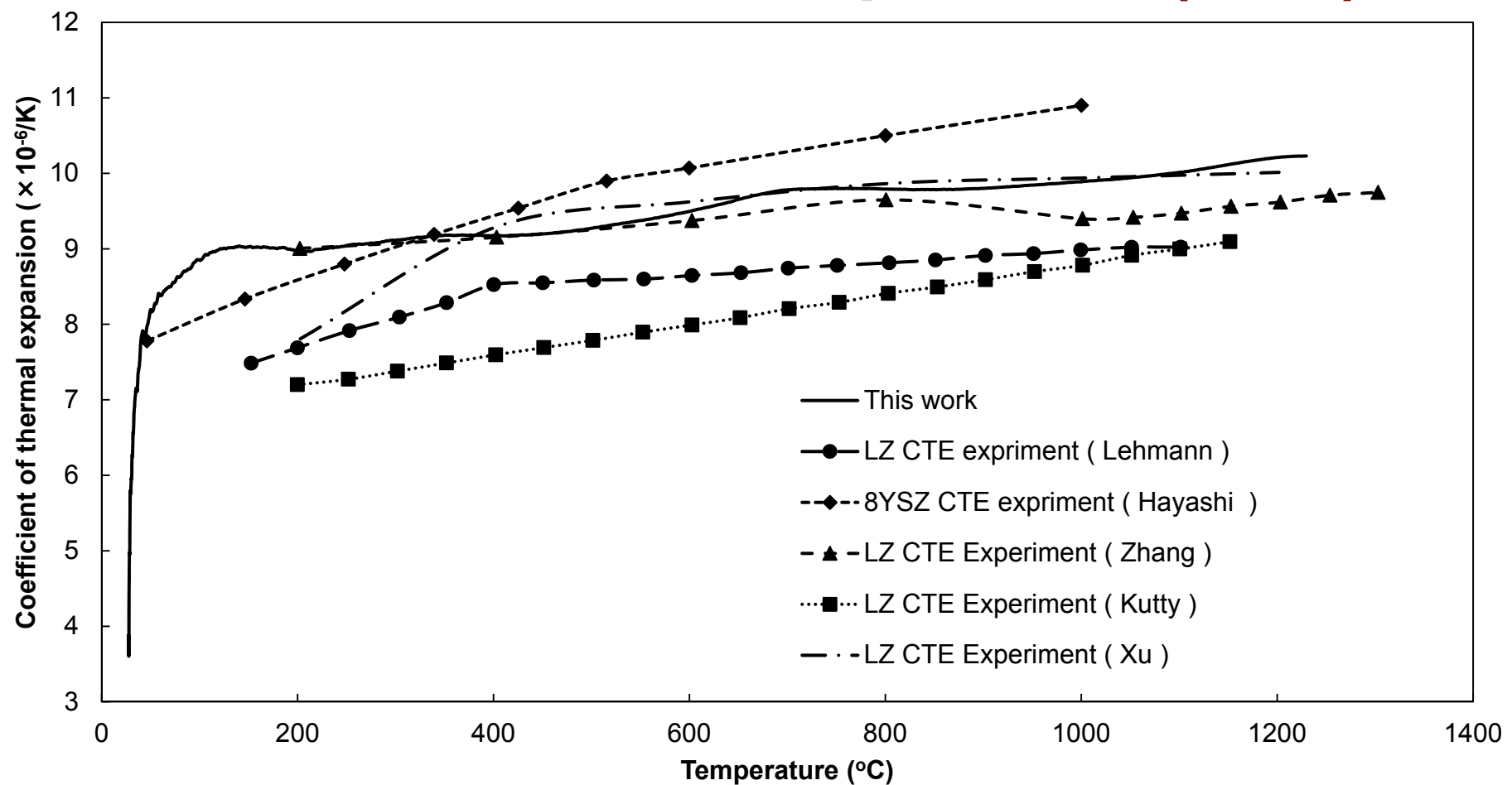
$$k = D_{th} \cdot C_p \cdot \rho$$

Thermal diffusivity is measured using laser flash diffusivity system (TA instrument DLF1200). Specific heat is measured by analytical method (TA instrument DLF1200)



Guo, et al., Thermal properties, thermal shock and thermal cycling behavior of lanthanum zirconate based thermal barrier coatings, *Metallurgical and Materials Transactions E*, (DOI: 10.1007/s40553-016-0070-4)

Coefficient of thermal expansion (CTE)



CTE is measured using a BAEHR dilatometer from 25 to 1400 $^{\circ}\text{C}$.

H. Lehmann, D. Pitzer, G. Pracht, R. Vassen, D. Stöver, Journal of the American Ceramic Society, 86 (2003) 1338-1344.

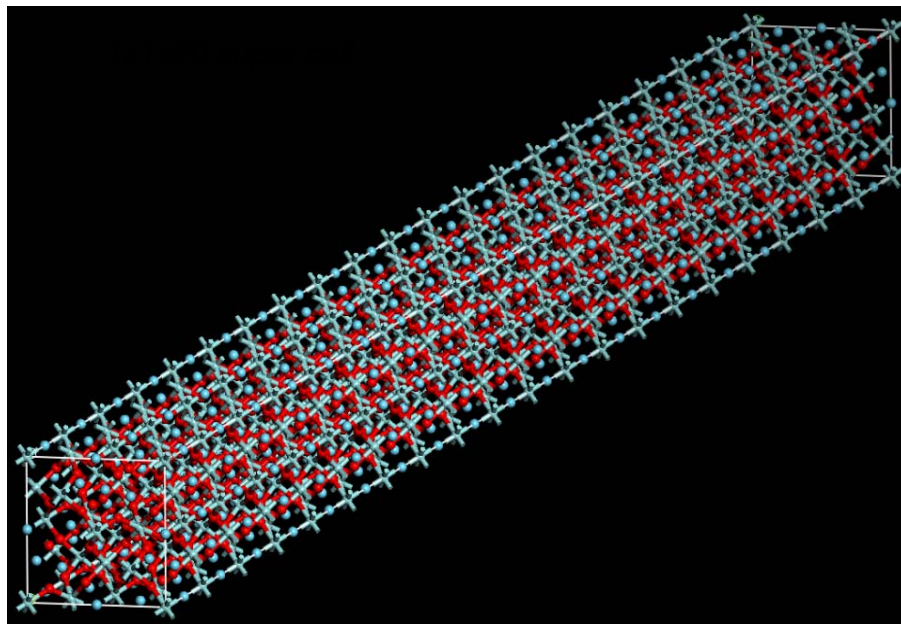
H. Hayashi, T. Saitou, N. Maruyama, H. Inaba, K. Kawamura, M. Mori, Solid State Ionics, 176 (2005) 613-619.

Guo, et al., Thermal properties, thermal shock and thermal cycling behavior of lanthanum zirconate based thermal barrier coatings, *Metallurgical and Materials Transactions E*, (DOI: 10.1007/s40553-016-0070-4)

Outline

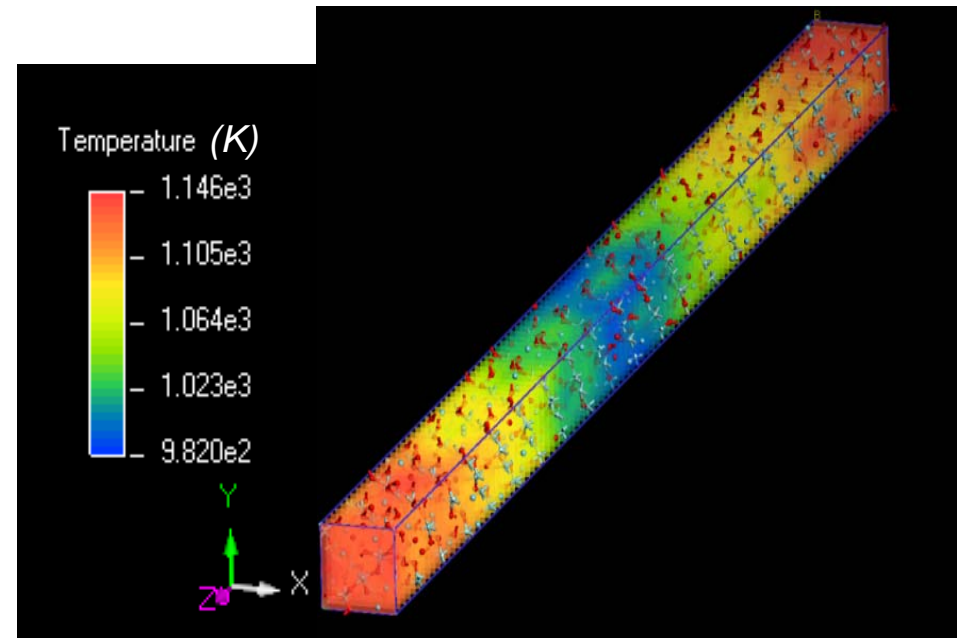
- Introduction
- Coating design and fabrication
 - Single ceramic layer (SCL) & Double ceramic layer (DCL) architectures
 - Composite coatings with buffer layers
- Characterization of physical and mechanical properties
 - Microstructure and composition
 - Porosity and hardness
 - Bond strength test
 - Erosion test
- **Characterization of thermal property and thermal durability**
 - Thermal conductivity, specific heat, coeff. of thermal expansion
 - Thermal shock (TS) test
 - Jet engine thermal shock (JETS) test
 - Furnace cycling thermal fatigue (FCTF) test
 - Thermal gradient mechanical fatigue (TGMF) test
- **MD&FE modeling of thermal conductivity;** DFT calculation of gas adsorption
- Summary and future work

$\text{La}_2\text{Zr}_2\text{O}_7$ thermal conductivity calculation



Replicate 20 conventional cells along the heat flow direction to form a super cell

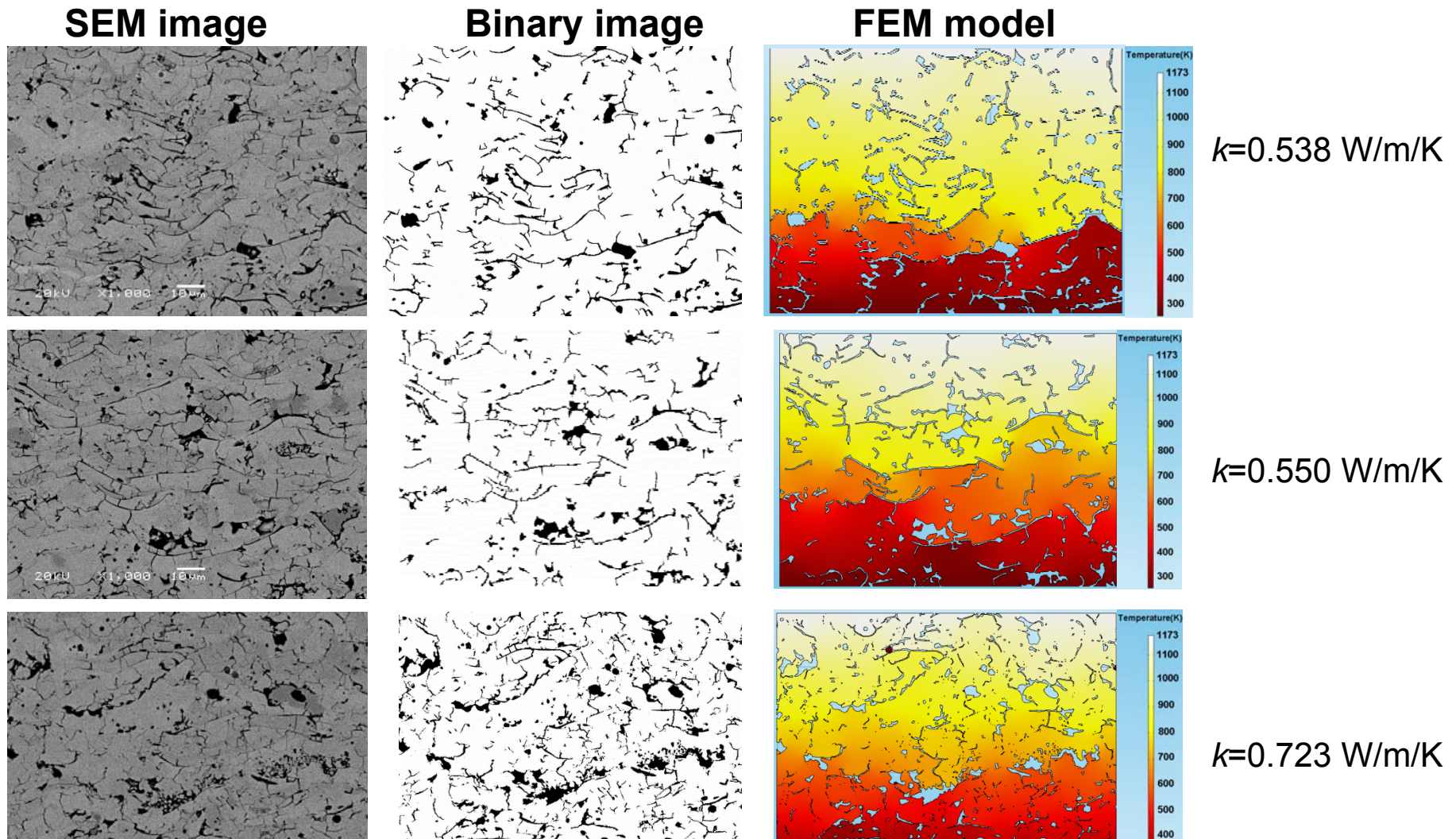
The calculated thermal conductivity is 1.2 W/m/K at the temperature of 1000 °C, which is reasonably in agreement with the experimentally measured thermal conductivity ~1.5 W/m/K [1].



Calculated temperature contour based on Fourier's law $k = -\vec{q''}/\vec{\nabla}T$

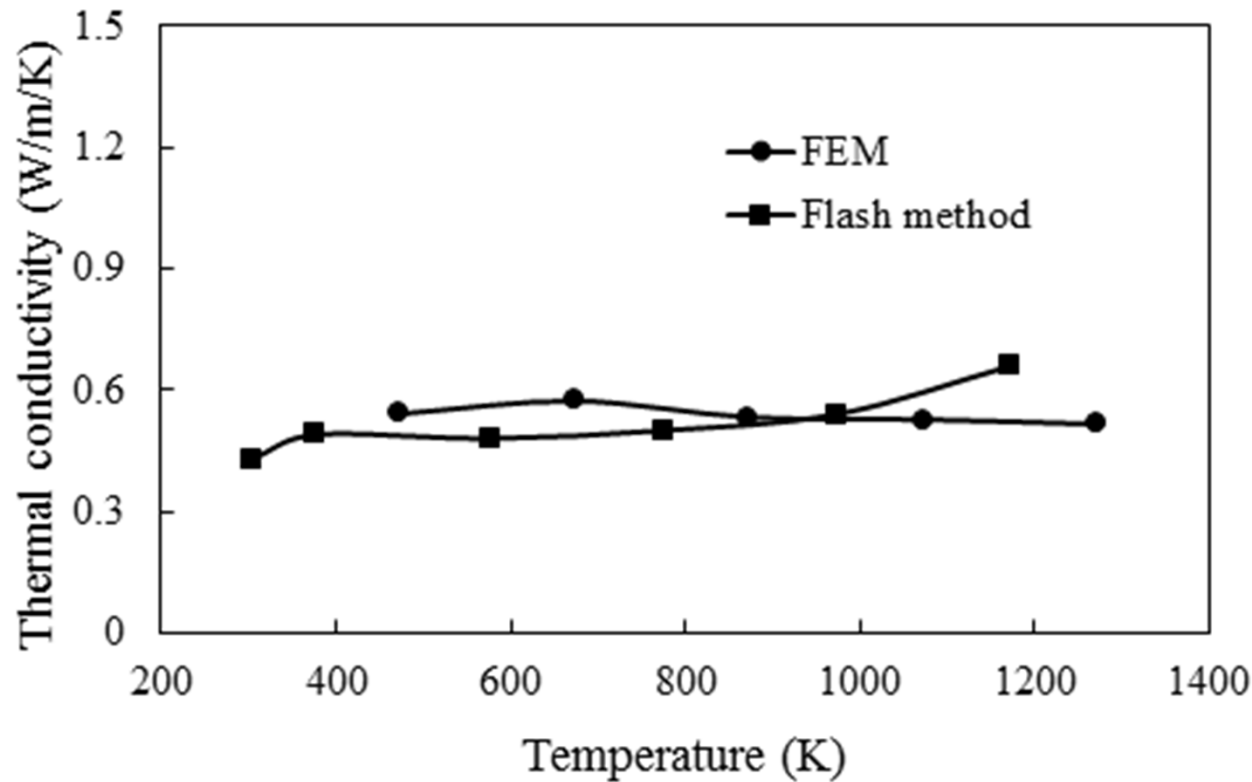
Guo, et al., Image-Based Multi-Scale Simulation and Experimental Validation of Thermal Conductivity of Lanthanum Zirconate, *International Journal of Heat and Mass Transfer*, (doi:10.1016/j.ijheatmasstransfer.2016.04.067)

Imaged based FEM calculation of thermal conductivity of $\text{La}_2\text{Zr}_2\text{O}_7$ TBC



Guo, et al., Image-Based Multi-Scale Simulation and Experimental Validation of Thermal Conductivity of Lanthanum Zirconate, *International Journal of Heat and Mass Transfer*, (doi:10.1016/j.ijheatmasstransfer.2016.04.067)

Imaged based FEM calculation of thermal conductivity of $\text{La}_2\text{Zr}_2\text{O}_7$ coating



Calculated thermal conductivity ~ 0.60 W/m-K, in good agreement with experimental data.

Guo, et al., Image-Based Multi-Scale Simulation and Experimental Validation of Thermal Conductivity of Lanthanum Zirconate, *International Journal of Heat and Mass Transfer*, (doi:10.1016/j.ijheatmasstransfer.2016.04.067)

Mapping thermal conductivity & heat capacity

Sample information

TBC:

Material: $\text{La}_2\text{Zr}_2\text{O}_7$

Thickness: $\sim 600\mu\text{m}$ (this is used in calculation)

Density: 90.55% dense, dense density=6 g/cc, so density $\rho = 5.478 \text{ g/cc}$

Specific heat: $c = 0.54 \text{ J/g-K} @ 1000\text{C}$

Substrate (following are room temperature properties obtained from matweb):

Material: Haynes 188

Density: $\rho = 8.98 \text{ g/cc}$

Thermal conductivity: $k = 10.4 \text{ W/m-K}$,

Specific heat: $c = 0.403 \text{ J/g-K}$, (therefore, $\rho c = 3.62 \text{ J/cm}^3\text{-K}$)

Thickness used in calculation: $L = 4 \text{ mm}$ (may have a small effect to results)

Test condition

Flash thermal imaging test with one flash lamp

Imaging speed: 994 Hz; imaging duration: 3 seconds

Thermal conductivity and heat capacity map

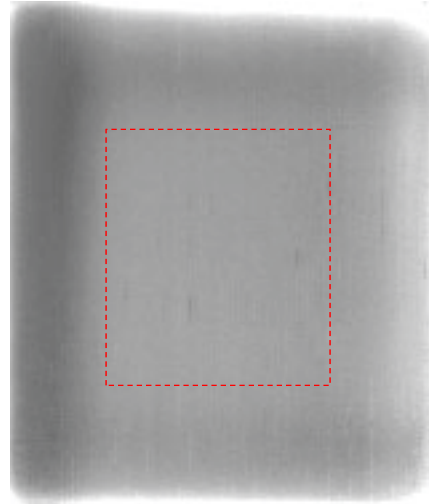


credit:
Jiangan Sun
@ ANL

TBC is 90.55% dense ($\rho=5.478\text{g/cc}$), with a nominal thickness of $600\mu\text{m}$
Indentation marks are from previous study

Mapping TBC thermal properties

Thermal conductivity k image



0 1 W/m-K

Heat capacity ρc image



0 2.5 J/cm³-K

credit:
Jiangan Sun
@ ANL

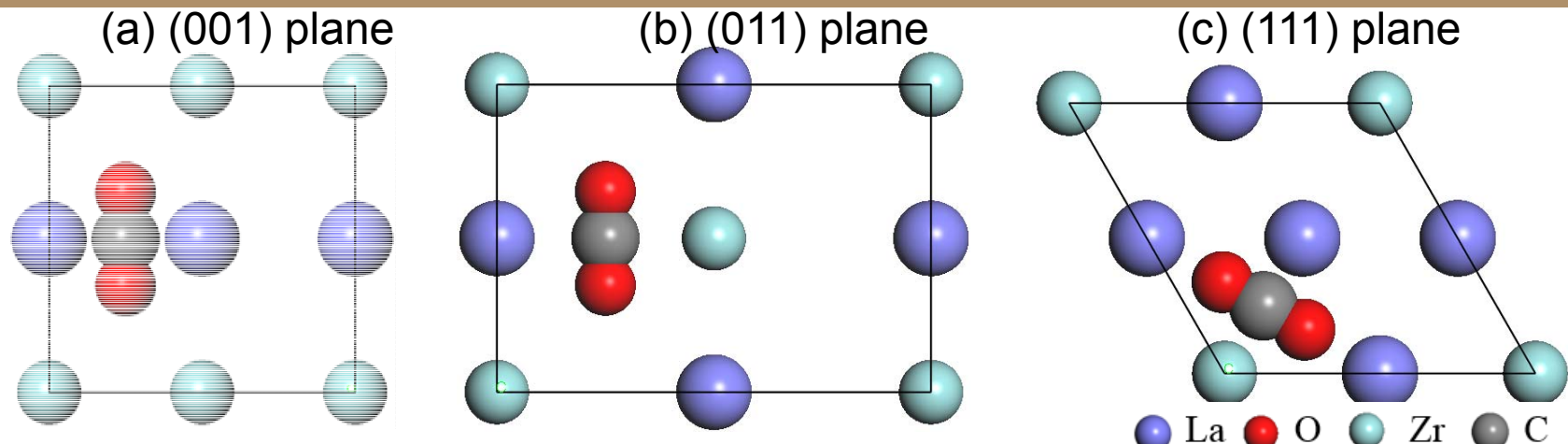
Predicted average TBC properties (within red rectangular area):
 $k = 0.55 \text{ W/m-K}$, $\rho c = 2.16 \text{ J/cm}^3\text{-K}$

- These results were based on a TBC thickness of 600 μm
- TBC specific heat @RT: $c = 0.393 \text{ J/g-K}$; predicted TBC density is: $\rho = \rho c / c = 2.16 / 0.393 = 5.5 \text{ g/cc}$

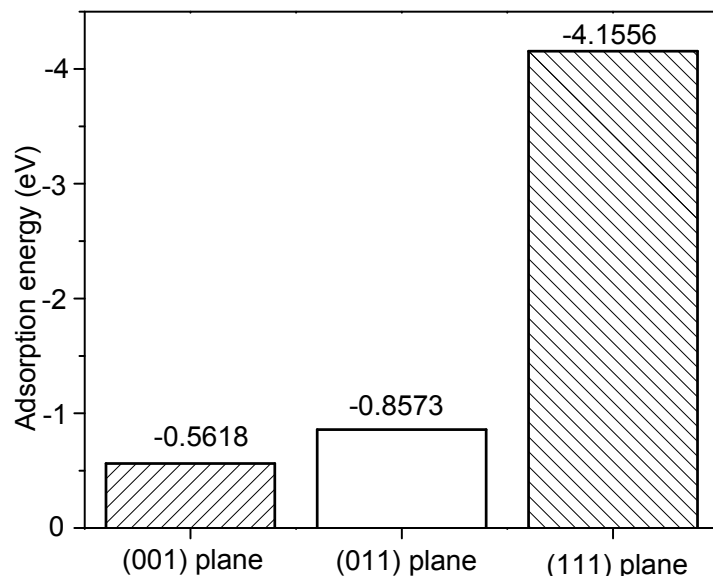
Outline

- Introduction
- Coating design and fabrication
 - Single ceramic layer (SCL) & Double ceramic layer (DCL) architectures
 - Composite coatings with buffer layers
- Characterization of physical and mechanical properties
 - Microstructure and composition
 - Porosity and hardness
 - Bond strength test
 - Erosion test
- **Characterization of thermal property and thermal durability**
 - Thermal conductivity, specific heat, coeff. of thermal expansion
 - Thermal shock (TS) test
 - Jet engine thermal shock (JETS) test
 - Furnace cycling thermal fatigue (FCTF) test
 - Thermal gradient mechanical fatigue (TGMF) test
- MD&FE modeling of thermal conductivity, **DFT calculation of gas adsorption**
- Summary and future work

CO_2 adsorption on coating surfaces



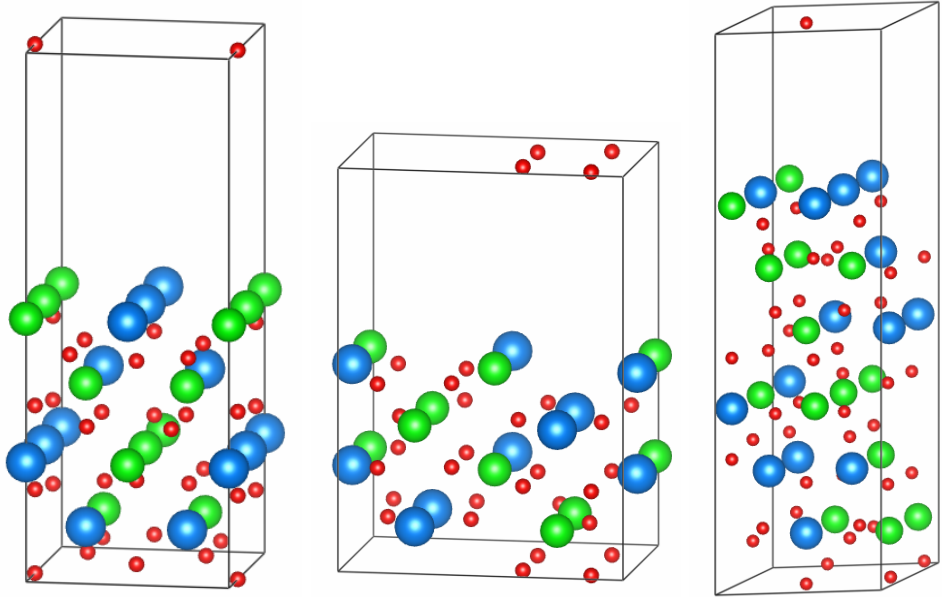
Top view of CO_2 adsorption sites on $\text{La}_2\text{Zr}_2\text{O}_7$ planes. Only $\text{La}_2\text{Zr}_2\text{O}_7$ top layer is shown



CO_2 is prone to be adsorbed on (111) plane, when the adsorption occurs in the bridge sites between La atom and Zr atom.

- Guo, et al., Carbon dioxide adsorption on lanthanum zirconate nanostructured coating surface: a DFT study, *Adsorption*, 22(2), pp 159-163, (2016)

O₂ adsorption on coating surfaces



(a)

(b)

(c)

La ₂ Zr ₂ O ₇ plane	A: bridge position (La-Zr) (eV)	B: 4-fold position (eV)	C: 3-fold-FCC position (eV)	D: 3-fold-HCP position (eV)
(001)	-3.5127	-5.1148	-	-
(011)	-5.0240	-1.3080	-	-
(111)	-3.5795	-	-5.5302	-3.8070

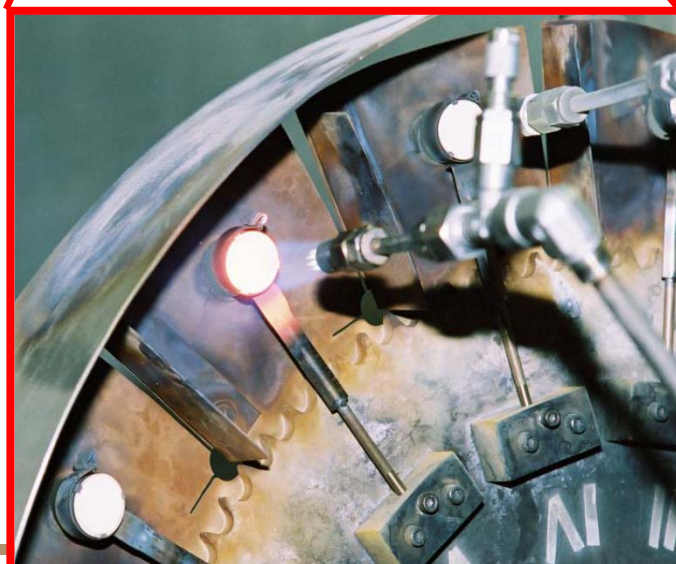
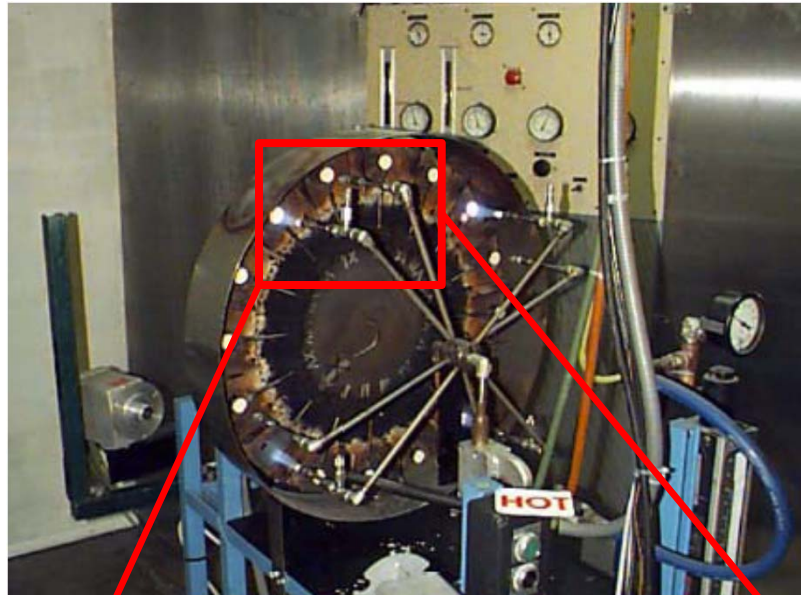
Computational slab models of various La₂Zr₂O₇ planes: (a) (001) plane, (b) (011) plane, and (c) (111) plane. The blue, green, and red balls indicate La atoms, Zr atoms, and O atoms, respectively.

The adsorption energies are exothermic. The lowest adsorption energy site is the 3-fold-FCC on (111) plane, confirmed by Bader charge transfer analyses.

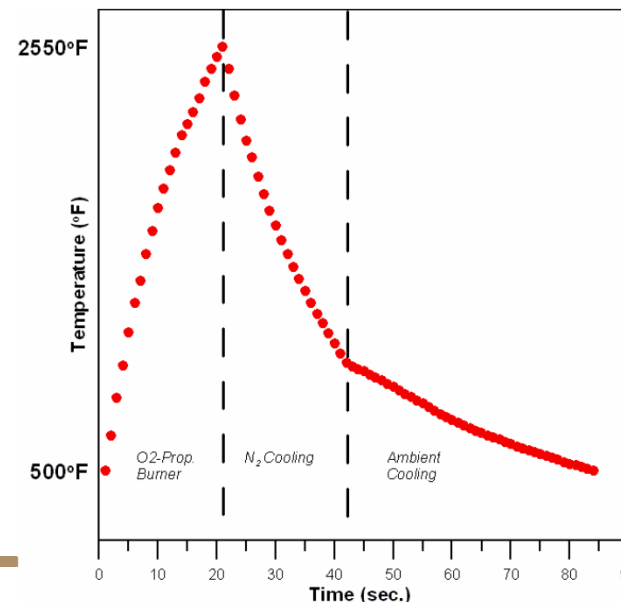
Outline

- Introduction
- Coating design and fabrication
 - Single ceramic layer (SCL) & Double ceramic layer (DCL) architectures
 - Composite coatings with buffer layers
- Characterization of physical and mechanical properties
 - Microstructure and composition
 - Porosity and hardness
 - Bond strength test
 - Erosion test
- **Characterization of thermal durability**
 - Thermal conductivity, specific heat, coeff. of thermal expansion
 - Thermal shock (TS) test
 - **Jet engine thermal shock (JETS) test**
 - Furnace cycling thermal fatigue (FCTF) test
 - **Thermal gradient mechanical fatigue (TGMF) test**
- MD&FE modeling of thermal conductivity; DFT calculation of gas adsorption
- Summary and future work

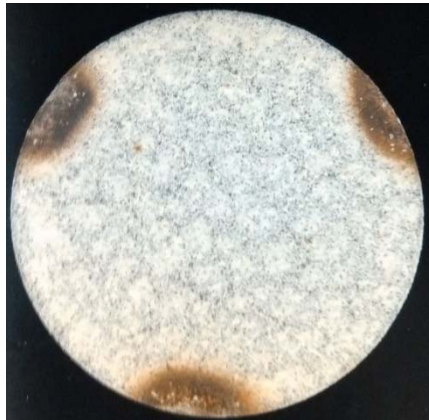
Jet engine thermal shock tests (JETS)



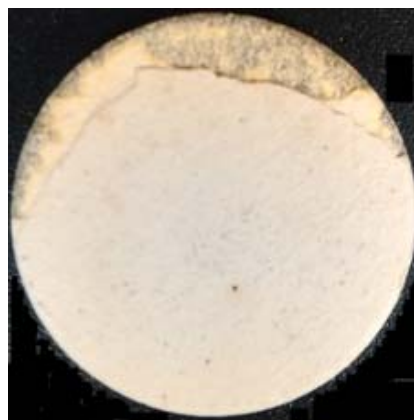
- Jet engine thermal shock (JETS) tests are conducted to investigate the thermal cycling performance.
- TBC samples are heated to 2250 °F (1232.2 °C) at the center for 20 s, and then cooled by compressed N₂ cooling for 20 s, and then ambient cooling for 40 s.
- Temperatures are measured by thermal couple and pyrometer.



Jet engine thermal shock test (JETS) results



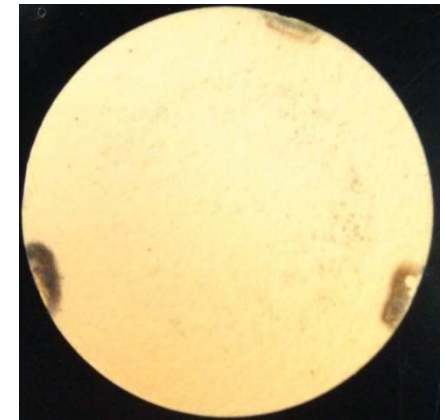
Single layer $\text{La}_2\text{Zr}_2\text{O}_7$



Porous 8YSZ + $\text{La}_2\text{Zr}_2\text{O}_7$



Dense 8YSZ + $\text{La}_2\text{Zr}_2\text{O}_7$

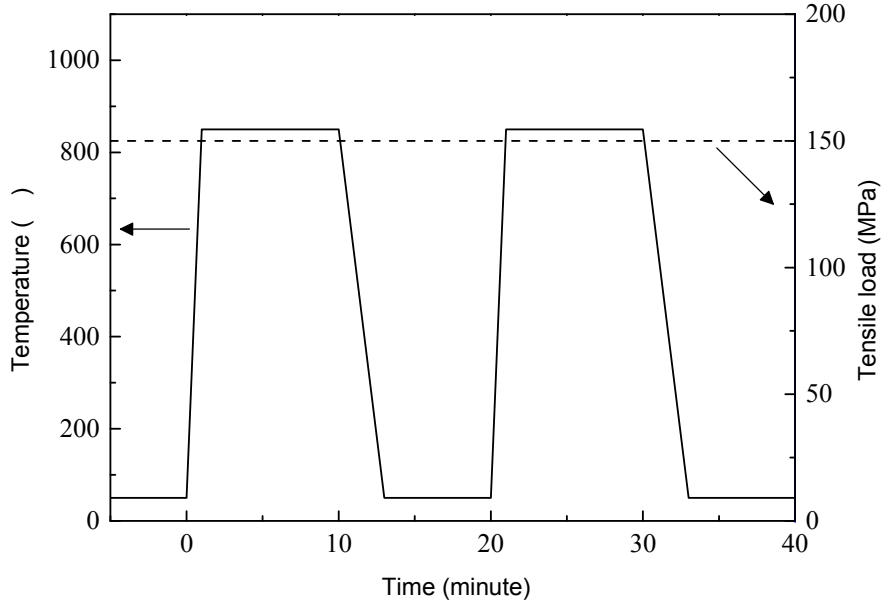
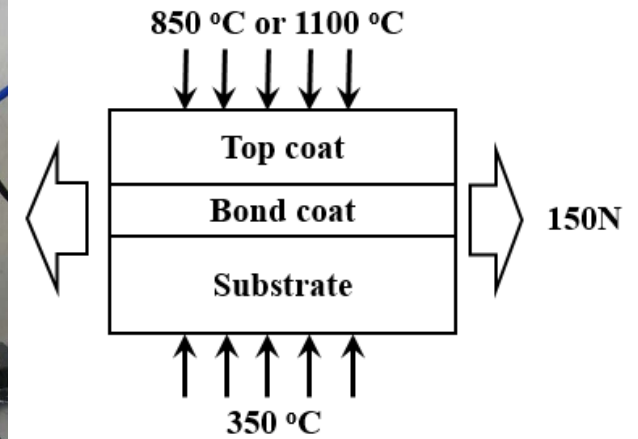
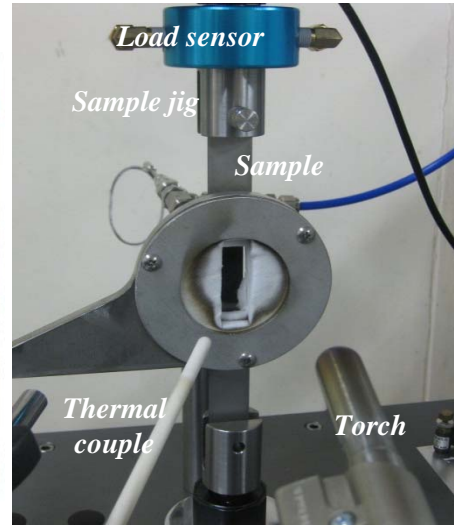


Porous 8YSZ

	Single-layer $\text{La}_2\text{Zr}_2\text{O}_7$	Porous 8YSZ + $\text{La}_2\text{Zr}_2\text{O}_7$	Dense 8YSZ + $\text{La}_2\text{Zr}_2\text{O}_7$	Single-layer porous 8YSZ
Number of cycles	25	> 2000	885	> 2000
Failure status	Complete delaminated	Edge delaminated	Complete delaminated	Intact

Guo, et al., Thermal properties, thermal shock and thermal cycling behavior of lanthanum zirconate based thermal barrier coatings, *Metallurgical and Materials Transactions E*, (DOI: 10.1007/s40553-016-0070-4)

Thermal gradient mechanical fatigue (TGMF)



At 850 °C

Sample	Test cycle
SCL porous 8YSZ	1200
DCL porous 8YSZ + La ₂ Zr ₂ O ₇	220
DCL dense 8YSZ + La ₂ Zr ₂ O ₇	50

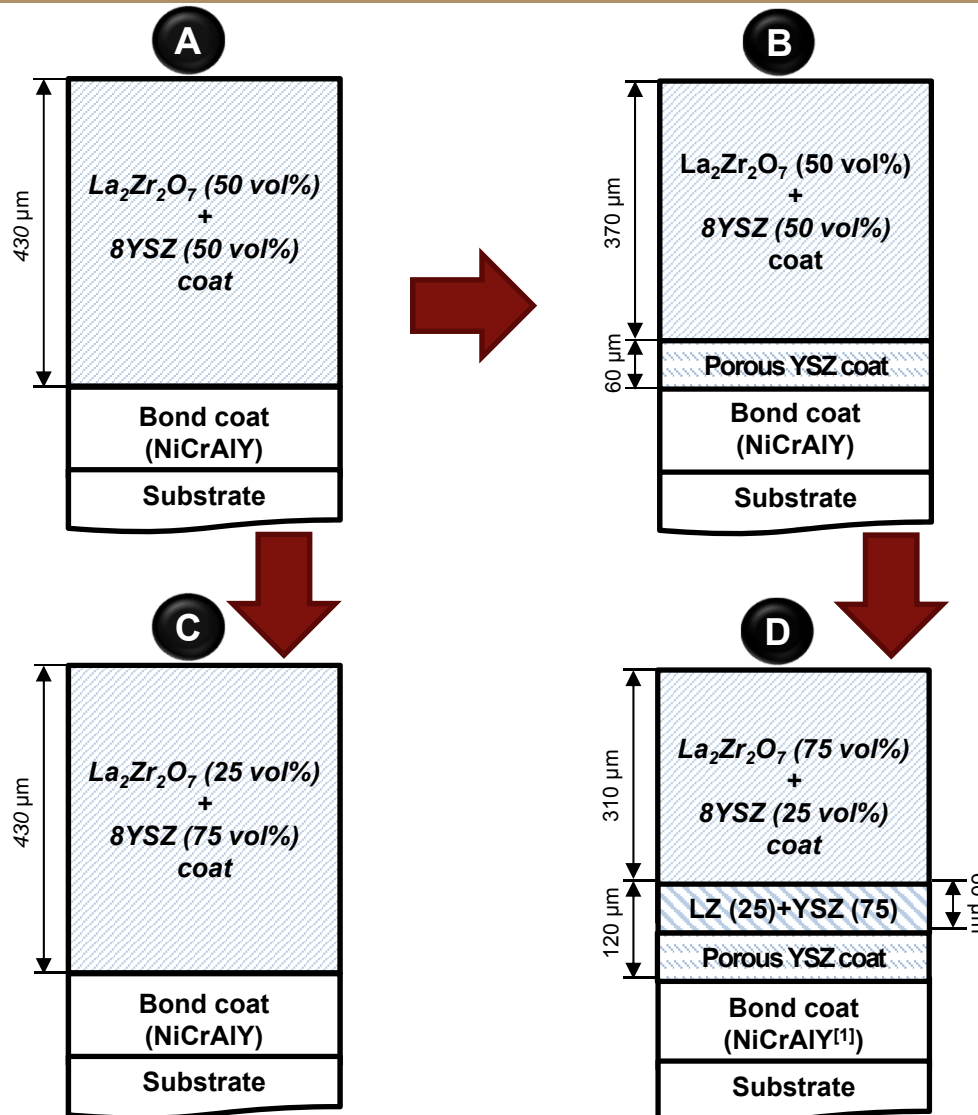
At 1100 °C

Sample	Test cycle
DCL porous 8YSZ + La ₂ Zr ₂ O ₇	38
DCL dense 8YSZ + La ₂ Zr ₂ O ₇	49

Outline

- Introduction
- **Coating design and fabrication**
 - Single ceramic layer (SCL) & Double ceramic layer (DCL) architectures
 - **Composite coatings with buffer layers**
- Characterization of physical and mechanical properties
 - Microstructure and composition
 - Porosity and hardness
 - Bond strength test
 - Erosion test
- Characterization of thermal property and thermal durability
 - Thermal conductivity, specific heat, coeff. of thermal expansion
 - Thermal shock (TS) test
 - Jet engine thermal shock (JETS) test
 - Furnace cycling thermal fatigue (FCTF) test
 - Thermal gradient mechanical fatigue (TGMF) test
- MD&FE modeling of thermal conductivity; DFT calculation of gas adsorption
- Summary and future work

Composite coatings with buffer layers



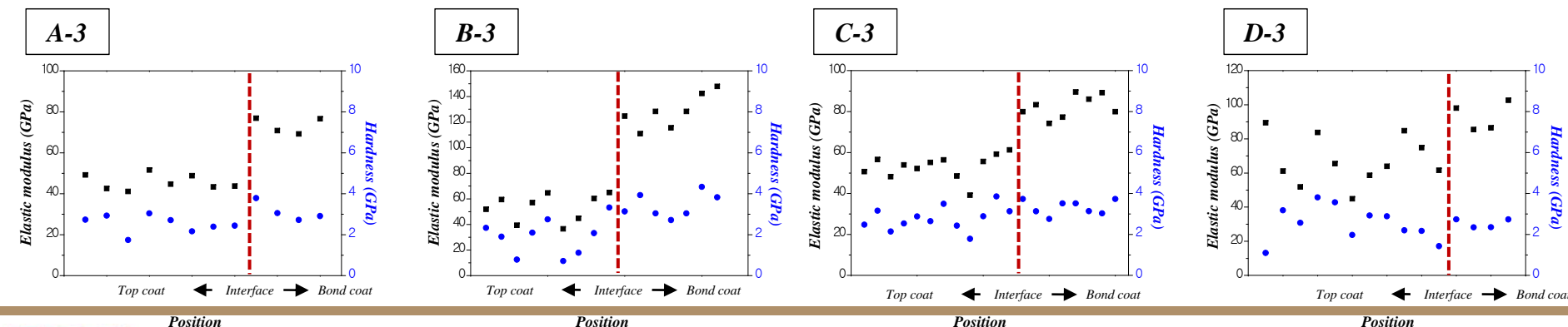
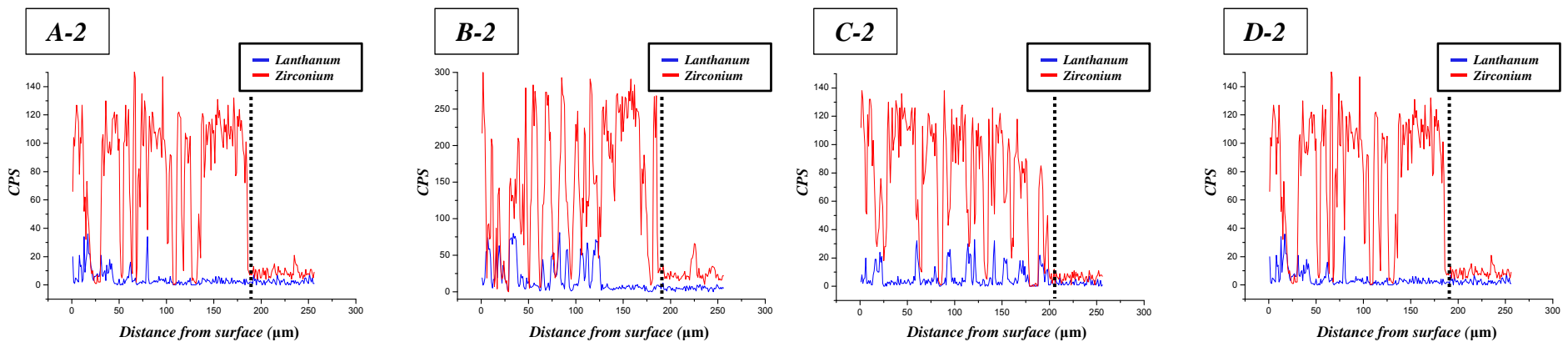
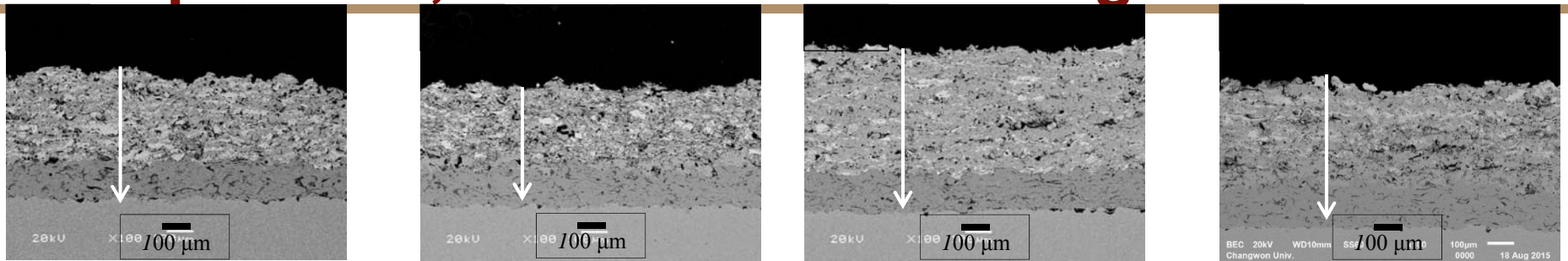
In order to improve the thermal durability in thermal cycling tests, new composite top coats are proposed:
thermal conductivity + matching CTEs

Introducing 1st buffer layer:
Increasing strain compliance
+ Decreasing CTEs mismatch

2nd buffer layer:
Further decrease CTEs mismatch

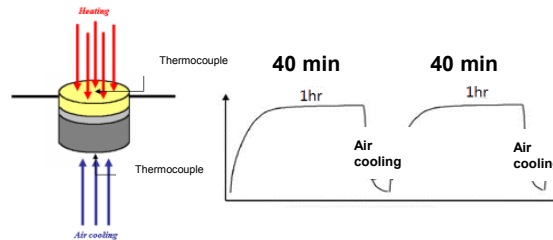
- Song, et al., Microstructure design for blended feedstock and its thermal durability in lanthanum zirconate based thermal barrier coatings, ICMCTF 2016

As-coated composite coatings: microstructure, composition, hardness and Young's modulus



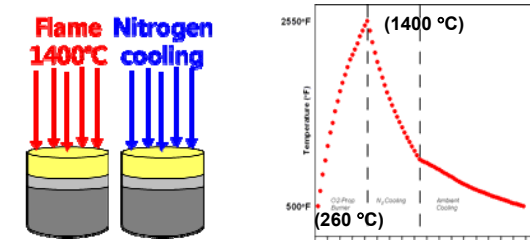
Thermal durability tests

Furnace cycling thermal fatigue (FCTF)



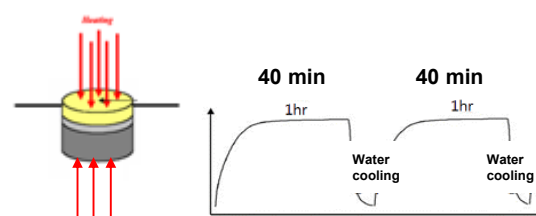
- Top surface temperature : ~ 1100 °C
- Bottom surface temperature : ~ 950 °C
- Heating time : 40 min
- Cooling type : Air & gas cooling

Jet engine thermal shock (JETS)



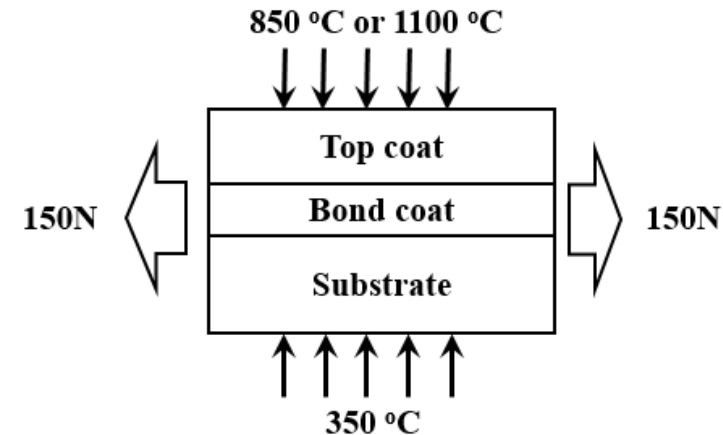
- Flame temperature : ~1400 °C
- Holding time : 20 sec
- Cooling time : 20 sec
- Cooling type : Nitrogen quenching

Thermal shock (TS)



- Heating temperature : ~ 1100 °C
- Heating time : 40 min
- Cooling type : Water quenching (30 °C)

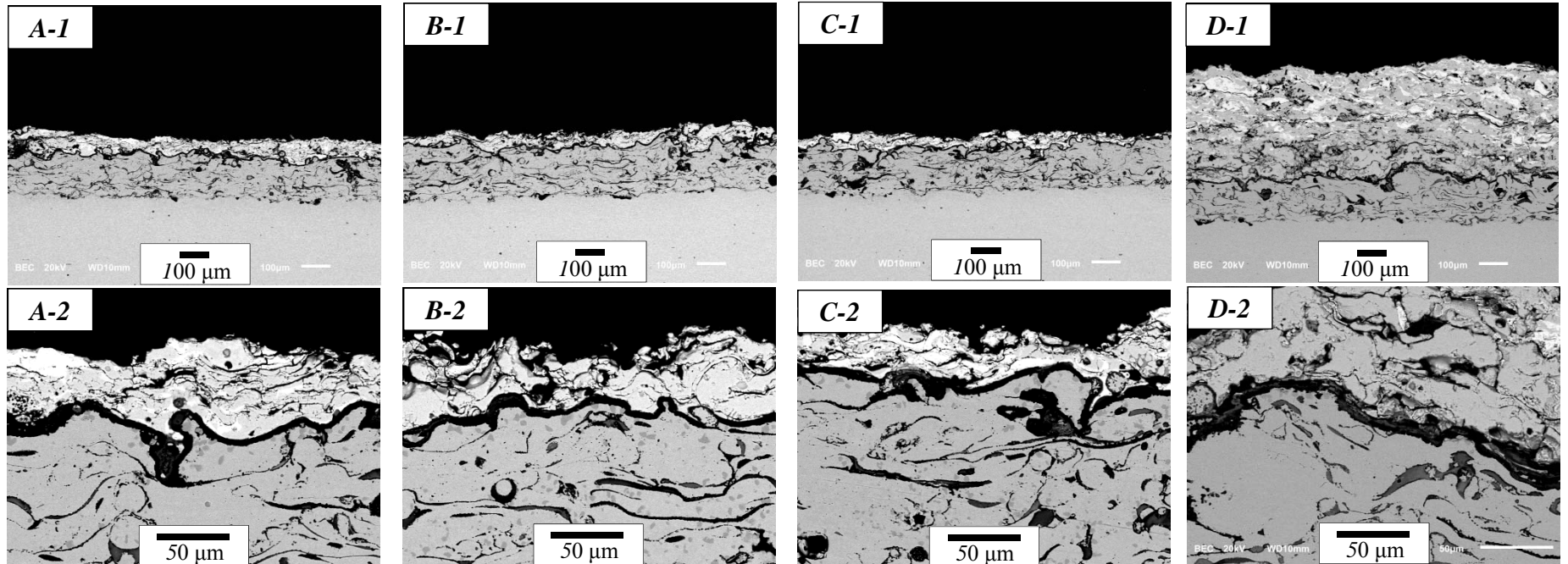
Thermal gradient mechanical fatigue (TGMF)



Thermal durability of composite coatings

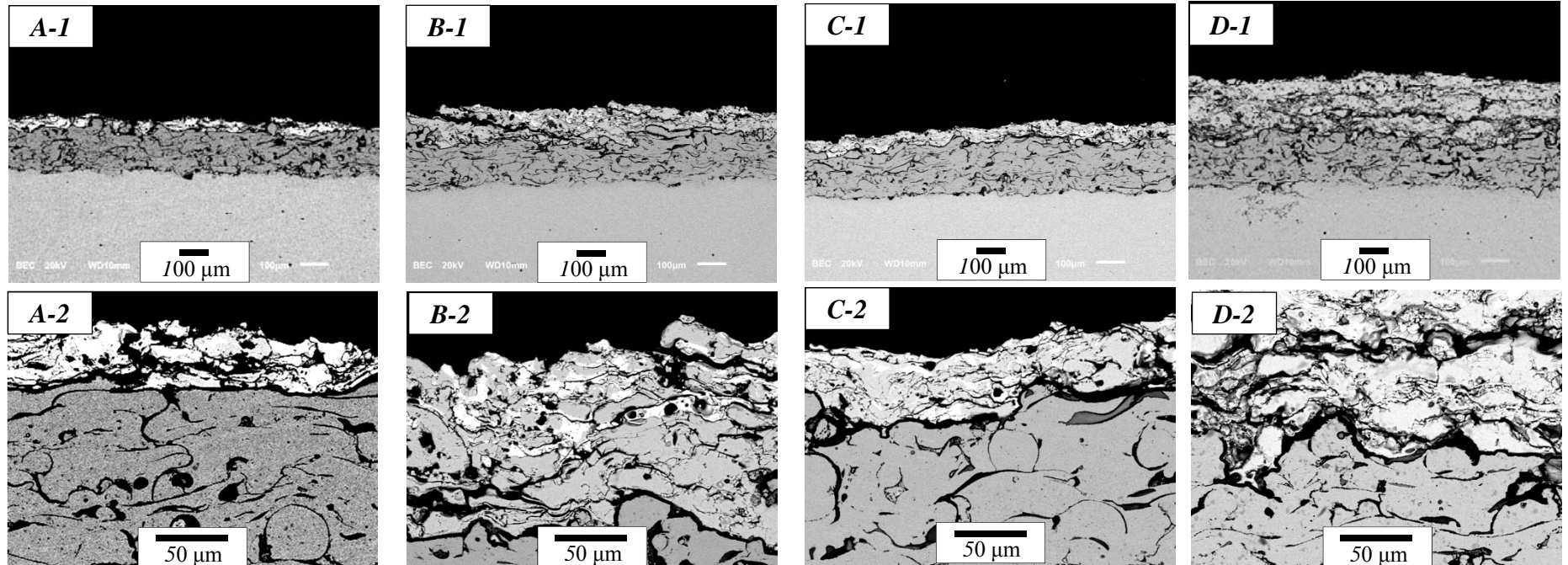
Sample species	FCTF test/Status	TS test/Status	JETS test/Status
(A) SLC TBC (50% LZ : 50 % YSZ in volume)	540 cycles/ Fully delaminated	10 cycles/ Fully delaminated	70 cycles/ Fully delaminated
(B) DLC TBC (50% LZ : 50 % YSZ in volume) with single buffer layer	768 cycles/ Fully delaminated	29 cycles/ Fully delaminated	2000 cycles/ Sound condition
(C) SLC TBC (25% LZ : 75 % YSZ in volume)	936 cycles/ Fully delaminated	14 cycles/ Fully delaminated	1022 cycle/ Fully delaminated
(D) DLC TBC (50% LZ : 50 % YSZ in volume) with double buffer layers	1143 cycles/ Sound condition	54 cycles/ Partially delaminated	2000 cycles/ Sound condition

Cross-sectional view after furnace cycling thermal fatigue (FCTF) test



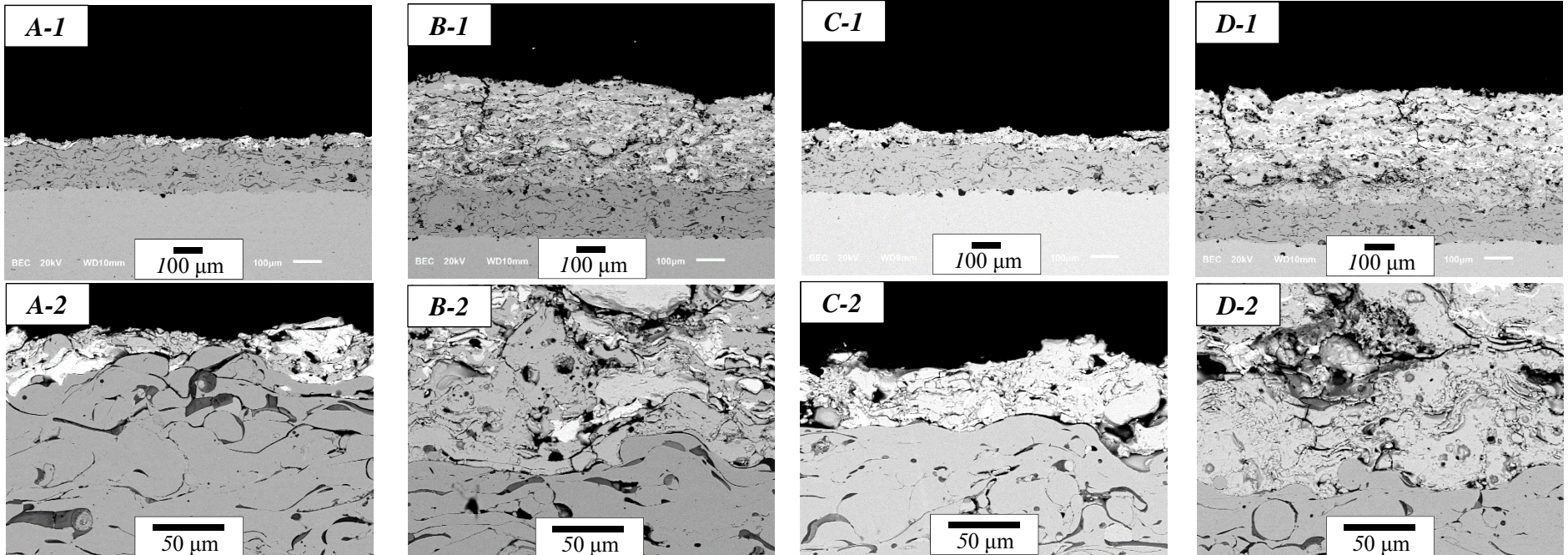
- Delamination within top coat and/or the interface between the top and bond coats in A, B, and C.
 - Thermally grown oxide (TGO) layer at interface between the top and bond coats in all samples
 - Spinel (Cr_2O_3 , NiAl_2O_4) in the TGO in D due to longer thermal exposure.
- Song, et al., Microstructure design for blended feedstock and its thermal durability in lanthanum zirconate based thermal barrier coatings, ICMCTF 2016

Cross-sectional view after thermal shock (TS) test



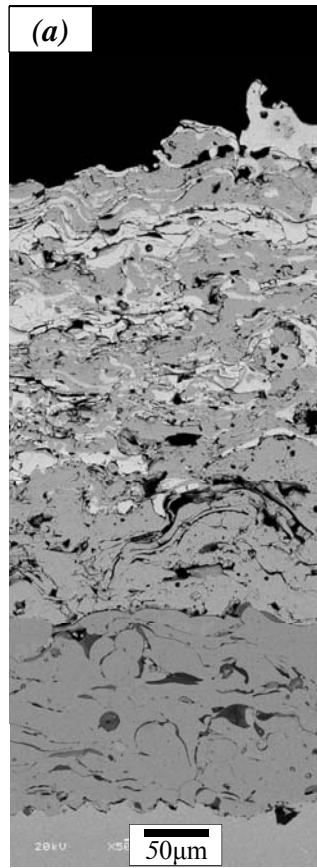
- In TS tests, A and C were delaminated less than 15 cycles, showing a thinner TGO layer than those in FCTF tests, due to CTE difference and low fracture toughness of LZ.
- B (survived 29 cycles, fully delaminated) and D (54 cycles, partially delaminated).

Cross-sectional view after jet engine thermal shock (JETS) test

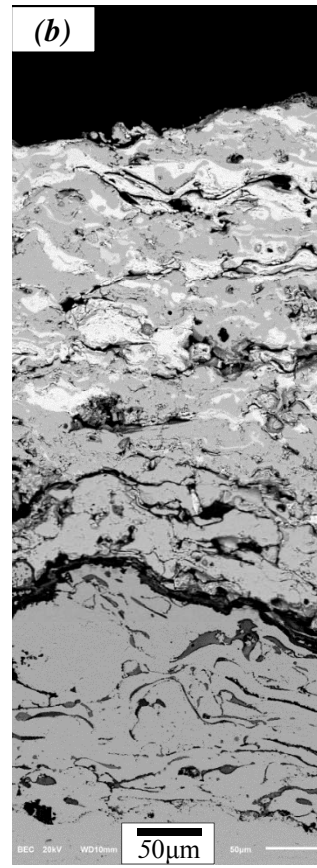


- A and C survived 70 and 1022 cycles, respectively.
- B and D survived 2000 cycles, showing a superior stability. (a) B and D showed vertical cracks during JETS test; (b) buffer layer(s); and (c) composite coats.

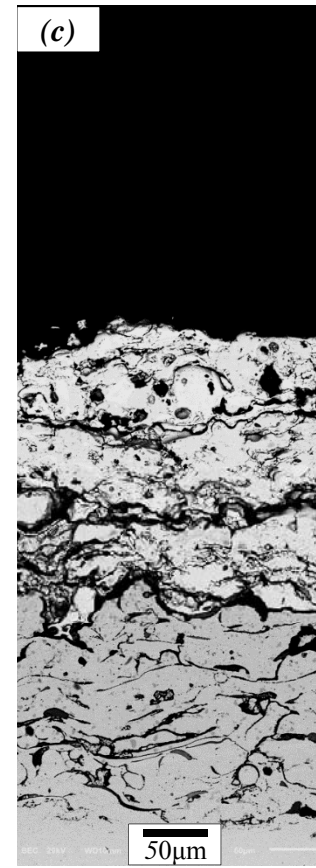
Composite coating with double buffer layers



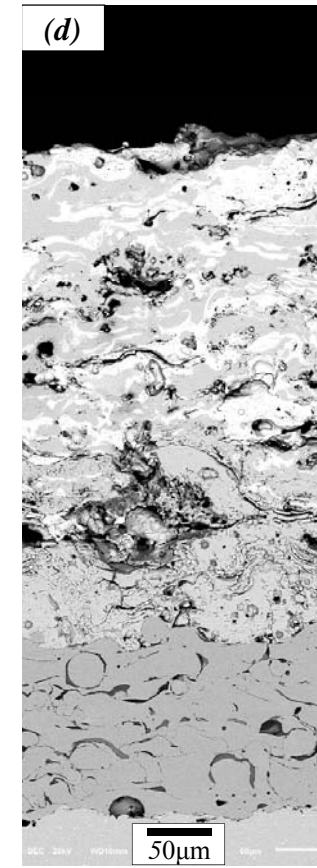
(a) as-coated



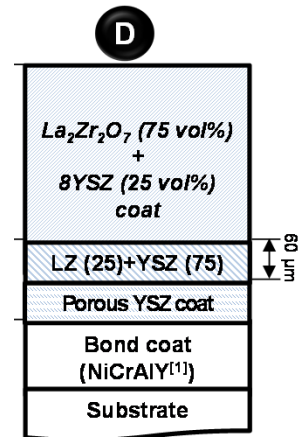
(b) after FCTF



(c) after TS

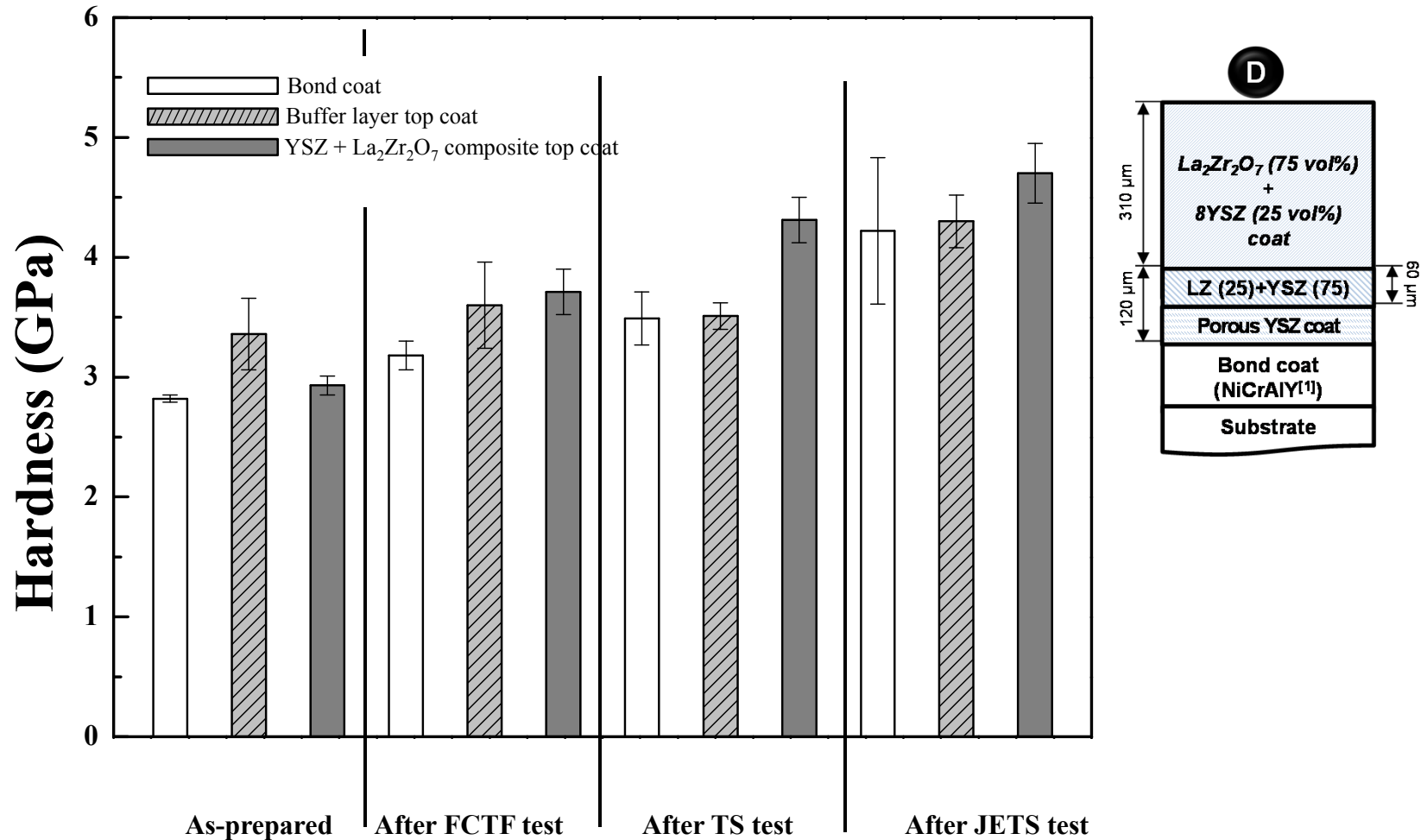


(d) after JETS



- Song, et al., Microstructure design for blended feedstock and its thermal durability in lanthanum zirconate based thermal barrier coatings, ICMCTF 2016

Vicker's hardness of composite coating with double buffer layers



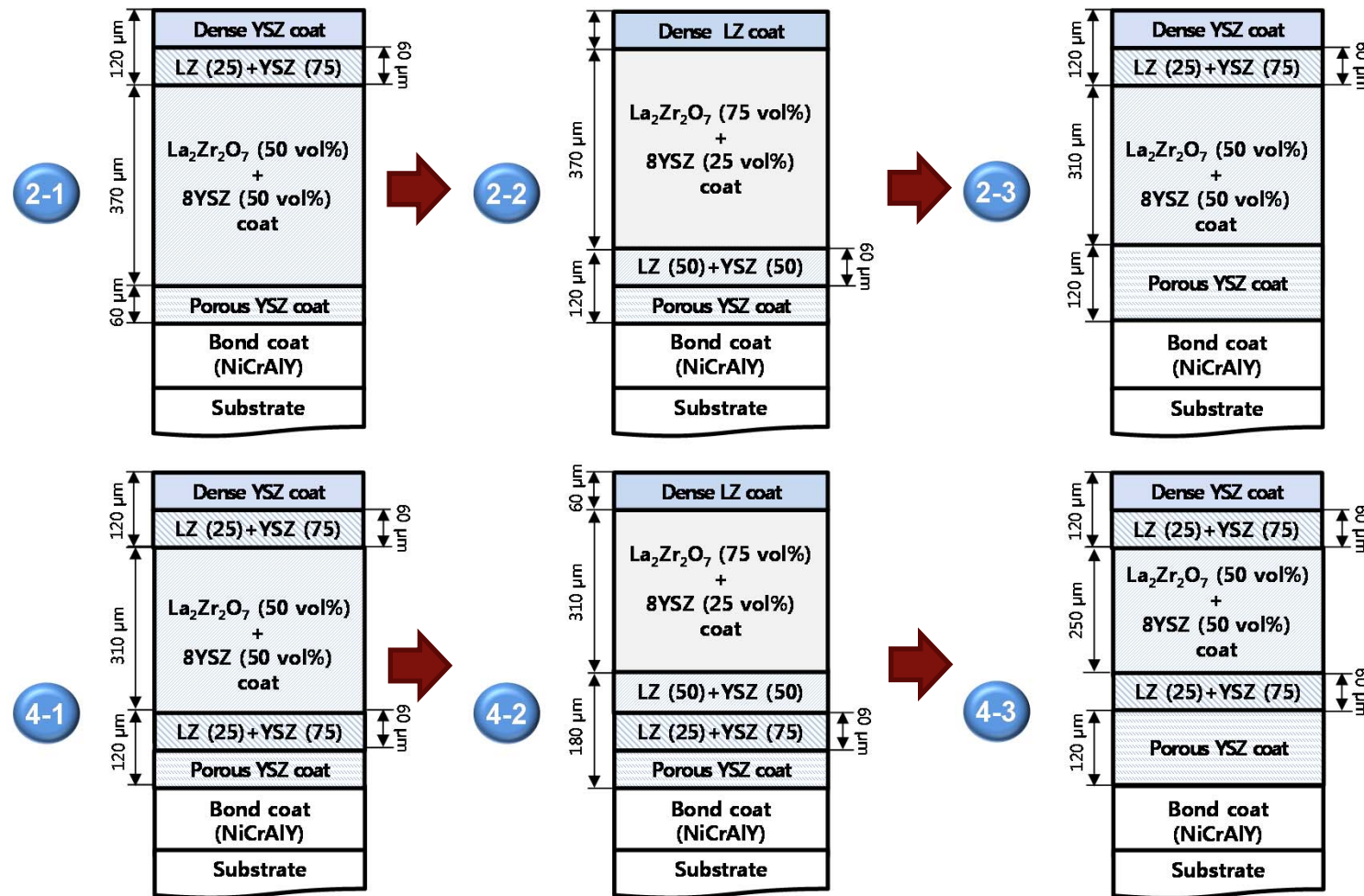
- In general, hardness increased due to densification in top coat and buffer layer, and oxidation of bond coat.

Summary

- $\text{La}_2\text{Zr}_2\text{O}_7$ powder and coating microstructure and chemistry characterizations show that $\text{La}_2\text{Zr}_2\text{O}_7$ is stable at high temperatures, which makes it suitable for TBC applications.
- Mechanical properties (hardness, bond strength) are similar to 8YSZ.
- Thermal conductivity of $\text{La}_2\text{Zr}_2\text{O}_7$ is lower than 8YSZ of similar porosity.
- Thermal properties using MD and image-based FE models calculations are in good agreement with experiments.
- Composite coatings and buffer layer are effective in improving the thermal durability of $\text{La}_2\text{Zr}_2\text{O}_7$ TBCs.
- TBC with double buffer layers showed the most outstanding thermal durability in all tests.

Future work

Thermal stability of $\text{La}_2\text{Zr}_2\text{O}_7$ coatings can be further improved by microstructure design using composite coating and buffer layers.



Publications and presentations

1. Xingye Guo, Linmin Wu, Yi Zhang, Yeongil Jung, Li Li, James Knapp, and Jing Zhang, Carbon Dioxide Adsorption on Lanthanum Zirconate Nanostructured Coating Surface: A DFT Study, *Adsorption*, 22(2), pp 159-163, 2016
 2. Xingye Guo, Zhe Lu, Yeongil Jung, Li Li, James Knapp, and Jing Zhang, Thermal properties, thermal shock and thermal cycling behavior of lanthanum zirconate based thermal barrier coatings, *Metallurgical and Materials Transactions E*, (DOI: 10.1007/s40553-016-0070-4)
 3. Xingye Guo, Linmin Wu, Yi Zhang, Yeongil Jung, Li Li, James Knapp, and Jing Zhang, First Principles Study of Nanoscale Mechanism of Oxygen Adsorption on Lanthanum Zirconate Surfaces, *Physica E*, (DOI: 10.1016/j.physe.2016.04.012)
 4. Xingye Guo, Bin Hu, Changdong Wei, Jiangang Sun, Yeon-Gil Jung, Li Li, James Knapp, and Jing Zhang, Image-Based Multi-Scale Simulation and Experimental Validation of Thermal Conductivity of Lanthanum Zirconate, *International Journal of Heat and Mass Transfer*, (DOI:10.1016/j.ijheatmasstransfer.2016.04.067)
 5. Dowon Song, Ungyu Paik, Xingye Guo, Jing Zhang, Zhe Lu, Je-Hyun Lee, Yeon-Gil Jung, Microstructure design for blended feedstock and its thermal durability in lanthanum zirconate based thermal barrier coatings, 2016 International Conference on Metallurgical Coatings and Thin Films (ICMCTF 2016), San Diego, CA, USA, April 25-29, 2016
 6. Xingye Guo, Zhe Lu, Yeon-Gil Jung, Li Li, James Knapp, Jing Zhang, Thermal and mechanical properties of novel lanthanum zirconate based thermal barrier coatings, 2016 International Thermal Spray Conference (ITSC 2016), Shanghai, China, May 10 - May 12, 2016
 7. Sung Hoon Jung, Zhe Lu, Seung Soo Lee, Yeon Gil Jung, Jing Zhang, Ungyu Paik, Microstructure design and thermal durability of Yb-Gd-YSZ thermal barrier coatings in cyclic thermal exposure, 2016 International Thermal Spray Conference (ITSC 2016), Shanghai, China, May 10 - May 12, 2016
 8. Xingye Guo, Linmin Wu, Yi Zhang, Yeon-Gil Jung, Li Li, James Knapp, Jing Zhang, Tensile Strength, Shear Strength and Adhesion Energy of Al₂O₃(0001) / Ni(111) Interface: A First Principles Study, *Materials Science & Technology* 2016 (MS&T16), Salt Lake City, UT, USA, October 23-27, 2016
-

9. Xingye Guo, Zhe Lu, Sung-Hoon Jung, Yeon-Gil Jung, Li Li, James Knapp, Jing Zhang, Microstructure Design of Novel Composite Lanthanum Zirconate-Yttria Stabilized Zirconia Based Thermal Barrier Coatings, Materials Science & Technology 2016 (MS&T16), Salt Lake City, UT, USA, October 23-27, 2016
10. Xingye Guo, Zhe Lu, Sung-Hoon Jung, Yeon-Gil Jung, Li Li, James Knapp, Jing Zhang, Thermal and mechanical properties of novel multi-layer lanthanum zirconate based thermal barrier coatings, Materials Science & Technology 2016 (MS&T16), Salt Lake City, UT, USA, October 23-27, 2016
11. Yi Zhang, Eun-Hee Kim, Geun-Ho Cho, Yeon-Gil Jung, Jing Zhang, Modeling mechanical properties of amorphous Na₂O-SiO₂ systems for high-temperature sand mold and core materials, Materials Science & Technology 2016 (MS&T16), Salt Lake City, UT, USA, October 23-27, 2016
12. Jing Zhang, Microstructure Design and Performance of Lanthanum Zirconate Based Thermal Barrier Coatings, Department of Materials Science, Purdue University, November 6, 2015
13. Xingye Guo, Jing Zhang, Yeon-Gil Jung, Li Li, James Knapp, Carbon Dioxide Adsorption on Nanostructured Lanthanum Zirconate Surface: A DFT study, IUPUI Nanotechnology Research Forum and Poster Symposium, Indianapolis, IN, October 23, 2015
14. Xingye Guo, Jing Zhang, Novel Lanthanum Zirconate Thermal Barrier Coatings For Gas Turbines, The Joint Board of Advisors Meeting, IUPUI, October 13th, 2015
15. Yeon-Gil Jung, Jing Zhang, Microstructure Design of Lanthanum Zirconate Coatings and Its lifetime Performance, The MS&T 2015, Material Science & Technology Conference and Exhibition, October 4 - October 8, 2015, Columbus, OH
16. Xingye Guo, Jing Zhang, Zhe Lu, Yeon-Gil Jung, Thermal Gradient Mechanical Fatigue Study of Lanthanum Zirconate Thermal Barrier Coatings, The MS&T 2015, Material Science & Technology Conference and Exhibition, October 4 - October 8, 2015, Columbus, OH
17. Xingye Guo, Jing Zhang, Density Functional Theory Study of Gas Adsorption on Lanthanum Zirconate Nanostructured Coating Surface, The MS&T 2015, Material Science & Technology Conference and Exhibition, October 4 - October 8, 2015, Columbus, OH
18. Yi Zhang, Jing Zhang, Sintering of Nanostructured Zirconia: A Molecular Dynamics Study, The MS&T 2015, Material Science & Technology Conference and Exhibition, October 4 - October 8, 2015, Columbus, OH

19. Dowon Song, Ungyu Paik, Jing Zhang, Zhe Lu, Je-Hyun Lee, Yeon-Gil Jung, Microstructure Design and Thermal Durability of Lanthanum Zirconate Based Thermal Barrier Coatings, 7th Asian Thermal Spray Conference (ATSC2015), Xi'an, China, September 23-25, 2015
20. Zhe Lu, Je-hyun Lee, Yeon-Gil Jung, Jing Zhang, Dowon Song, Ungyu Paik, Microstructure Evolution and Durability of Thermal Barrier Coatings in Thermally Graded Mechanical Fatigue Environments, 7th Asian Thermal Spray Conference (ATSC2015), Xi'an, China, September 23-25, 2015
21. Jing Zhang, Advanced Materials Research, Argonne National Laboratory, September 11, 2015
22. Yeon-Gil Jung, Zhe Lu, Ungyu Paik, and Jing Zhang, Lifetime Performance of Thermal Barrier Coatings in Thermally Graded Mechanical Fatigue Environments, The 11th International Conference of Pacific Rim Ceramic Societies(PacRim-11), Jeju, Korea, August 30 - September 4, 2015
23. Yeon-Gil Jung, Zhe Lu, Qi-Zheng Cui, Sang-Won Myoung, and Jing Zhang, Thermal Durability and Fracture Behavior of Thermal Barrier Coatings in Thermally Graded Mechanical Fatigue Environments, the International Symposium on Green Manufacturing and Applications 2015 (ISGMA 2015), Qingdao, China, June 23 - June 27, 2015
24. Jing Zhang, Yeon-Gil Jung (eds.), 1st International Joint Mini-Symposium on Advanced Coatings, Materials Today: Proceedings, 2014
25. Xingye Guo, Jing Zhang, Zhe Lu, Yeon-Gil Jung, Theoretical prediction of thermal and mechanical properties of lanthanum zirconate nanocrystal, the 1st International Conference & Exhibition for Nanopia, Changwon Exhibition Convention Center, Gyeongsangnam-do Province, Miryang City, Korea, November 13-14, 2014
26. Sang-Won Myoung, Zhe Lu, Qizheng Cui, Je-Hyun Lee, Yeon-Gil Jung, Jing Zhang, Thermomechanical properties of thermal barrier coatings with microstructure design in cyclic thermal exposure, the 1st International Conference & Exhibition for Nanopia, Changwon Exhibition Convention Center, Gyeongsangnam-do Province, Miryang City, Korea, November 13-14, 2014
27. Zhang, J., X. Guo, Y.-G. Jung, L. Li, and J. Knapp, Microstructural Non-uniformity and Mechanical Property of Air Plasma-sprayed Dense Lanthanum Zirconate Thermal Barrier Coating. Materials Today: Proceedings, 2014. 1(1): p. 11-16.
28. Guo, X. and J. Zhang, First Principles Study of Thermodynamic Properties of Lanthanum Zirconate. Materials Today: Proceedings, 2014. 1(1): p. 25-34.